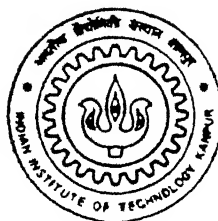# POWDER METALLURGY PROCESSING & PROPERTIES O IRON ALUMINIDE-IRON-IRON ALUMINIDE AND COPPER-IRON-COPPER LAMINATED COMPOSITE STRIPS

By

S. B. VENKATA GIRIDHAR
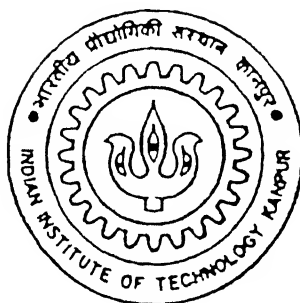
TH
MME/ 1998/ M
G 443p

DEPARTMENT OF MATERIALS & METALLURGICAL ENGINEERING

INDIAN INSTITUTE OF TECHNOLOGY, KANPUR

DECEMBER, 1998

POWDER METALLURGY PROCESSING & PROPERTIES OF IRON ALUMINIDE-IRON-IRON ALUMINIDE AND COPPER-IRON-COPPER LAMINATED COMPOSITE STRIPS

*A Thesis Submitted
In Partial Fulfillment of the Requirements
for the Degree of*

MASTER OF TECHNOLOGY

by

S.B. VENKATA GIRIDHAR

to the

**DEPARTMENT OF MATERIALS & METALLURGICAL ENGINEERIN
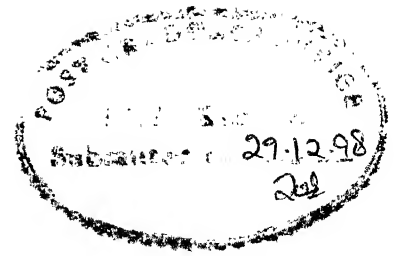INDIAN INSTITUTE OF TECHNOLOGY
KANPUR - 208016 INDIA
DECEMBER 1998**

CERTIFICATE

This is to certify that the work contained in the thesis entitled **"POWDER METALLURGY PROCESSING & PROPERTIES OF IRON ALUMINIDE-IRON-IRON ALUMINIDE AND COPPER-IRON-COPPER LAMINATED COMPOSITE STRIPS"**, by S.B. VENKATA GIRIDHAR   has been carried out under my supervision and that this work has not been submitted elsewhere for a degree.

Dr. R.K. DUBE

Professor

Department of Mat. & Met. Engineering

December, 1998   I.I.T., Kanpur

ABSTRACT

Powder Metallurgy processing of laminated Metal-Intermetallic and Metal-Metal composite strip based on Iron aluminide-Iron and Cu-Fe systems has been carried out. The Fe-Al intermetallic with Fe_3Al composition was prepared by mechanical alloying of Fe and Al powders. Laminated composite compacts of Fe_3Al-Fe-Fe_3Al and Cu-Fe-Cu were prepared by hot pressing the powders. Laminated strips of ~1mm thickness are prepared by hot rolling the hot pressed composite compacts. The physical and mechanical properties together with the microstructure of the laminated composite strips are studied. In case of Fe_3Al-Fe-Fe_3Al laminated composite strips the tensile strength and ductility was found out to be poor because of poor interfacial bonding between iron and iron aluminide which leads to delamination during tensile testing. The ultimate tensile strength values of Cu-Fe-Cu laminated strip was found out to be satisfactory. Where as the elongation value is very less which is probably attributed to the presence of some brittle phase at the interface leading to the problem of delamination. The mechanical properties in particular percentage elongation can be improved upon by introducing a thin nickel layer in between iron and copper layers.

ACKWNOLEDGEMENTS

Contents

List of Tables

List of Figures

Chapter 1

INTRODUCTION

Bonded metal laminates are a unique form of composites which consists of alternating metal or metal containing layers, bonded together with discrete interfaces. These materials represent a unique laminated or layered composite form that should be distinguished from graded materials, which have diffuse interfaces, or layered materials, which can consists of alternating layers of a wide range of materials including metal/metal, metal/ceramic, ceramic/ceramic or intermetallic/metal combinations.

Today, bonded metal laminates are employed in incresing volume and in more and more diverse field, because

1. they combine the properties of their component parts to obtain composite properties which may be new or unique, or

2. they make it easier or less costly to obtain certain properties than is possible with 'solid' materials.

These laminates can dramatically improve many properties including frcture toughness, fatigue behaviour, impact behaviour, wear, corrosion and damping capacity or provide enhanced formability or ductility for otherwise brittle materials. By controlling factors such as volume percent of the component materials, layer thickness and processing history, laminates can be engineered to produce a material with prescribed properties.

The idea of laminates has been known from antiquity (1500 B.C.). Early examples of laminates include glude wood, in the form of parallel-laminated members and plywood.

Such combinations of several layers of wood are found in a variety of ancient Egyptian items. The greatly incresed use of plywood and its applications to engineering structure is, however, a recent phenomenon, largely made possible by improved synthetic adhesives. There was evidence that, at around 400 B.C., the greek black smiths made a laminated metal composite, which consists of medium carbon steel cutting blade adjoining the low carbon backing plate.

In more recent times, begining in the period around AD 500, pattern welded daggers and swords were made. Included in this group of materials are the Norwegian (Viking) blades, the Chainese welded swords, and the Japanese sword. Even though, there is a large improvement in the processing technology from the ancient times, till date virtually no bonded metal laminates have become commercially available that use these materials for their unique structural properties.

Laminate Forms and Processing

Bonded metal laminates can be made by many techniques, which may be categorised roughly into three groups - bonding, deposition and spray forming. Bonding techniques start with component materials in sheet, plate or powder form that are then solid state bonded at the interface. In the case of deposition techniques, layers of component materials are formed sequentially by atomic or molecular scale transport of the component materials. Spray forming techniques, involves direct deposition of molten metals of the component material into a laminate form [1].

Bonded Laminates

Bonding techniques: Bonding techniques may be classified into several sub groups, such as, adhesive bonding, melt bonding, infiltration, diffusion bonding, reaction bonding and deformation bonding. Surface preparation of the component materials, bonding temperature, pressure and time, inter diffusion and chemical reaction between the component materials greatly influences the microstructure, bond strength at the interface and overall physical and mechanical properties of the resulting laminate.

Adhesive Bonding:

Early versions of Aluminum laminates were bonded with epoxy adhesives which resulted in an extremely high interfacial bond strength. The bonds could be made so strong that the laminates did not delaminate when pulled to failure. A variation of this adhesive bonding method resulted in the commertial products **ARALL** (aramid fibre reinforced epoxy) and **GLARE** (glass fibre reinforced epoxy). In these cases the adhesive between the aluminum layers is reinforced with strong Kevlar or glass fibres.

Melt Bonding:

The component materials (in the form of sheet or plate) were dipped in the molten metal and pressure is applied during the process of withdrawl, so that the liquid metal will solidify and produces a good bonding.

Infiltration:

The multilayered laminate is heated upto the melting point of one of the component material, so that the infiltration will takes place. This technique is helpful, if one of the material in the laminate having low melting point.

Diffusion Bonding:

The component materials in the form of sheet, plate or powder were stacked together in a hot press and heated to near the solutionizing temperature. A low pressure, less than that required for large scale plastic flow, was appiled to facilitate diffusion bonding.

Reaction Bonding:

The component materials of the laminate were stacked and heated under pressure, so that a new phase will form. By adjusting the relative thickness of the layers, we can produce a large variety of new phases. This method is widely used for the preparation of iron/nickel aluminides from the elementary metals [2].

Deformation Bonding:

In deformation bonding layers of the component materials are stacked and subjected to large plastic deformation until they are bonded together. Deformation bonding is a most effitient technique from the industrial processing view point. This includes press, roll and explosive bonding as well as coextrusion. The first three deformation bonding techniques are used for making laminates in plate or sheet form,and the fourth technique is used for producing laminates of rod shape [3].

Deposited Laminates

Deposition technique involves atomic or molecular scale transport of the component materials such as sputtering, evaporation chemical or physical vapour deposition (**CVD** or **PVD**) or electro plating. With the exception of plating technique, many of the deposition methods are probably too slow and costly to be practical for making large scale, load bearing components.

Spray Formed Laminates

Spray forming is a process for applying layers of metal or ceramic to a substrate. A *'gun'* is used in which either a combustion flame or a plasma flame melts and propels the material in finely divided form towards the article to be covered. Standered spray formed materials includes numerous steels, aluminum, zinc, copper, carbides, oxides such as aluminum oxide and zirconium oxide and refractory materials including molybdenum and tungstun. This process can be used for the formation of laminates having a substrate and atleast one coating material. Very often the laminate is more complex, having several types of spray formed layers [4].

Chapter 2

LITERATURE REVIEW

2.1 *P/M* Processing of Laminated Composites

Powder metallurgy is a versatile technology of material processing. It has all the right ingredients : economy in raw materials and energy combined with a flexibility in the final shape of products with desirable properties. Many of the powder metallurgical techniques are equally applicable to non metals as to metals [5]. Powder metallurgy provides flexible processes for manufacturing composites with tailored microstructure. With the wide range of powder variables and process variables, it is possible to design microstructures in such a manner as to obtain specific properties at specific location in the component.

There are numerous techniques available for the preparation of the laminated composites via powder metallurgical route. A few of them are roll compaction, cold compaction, cold isostatic pressing, hot pressing, hot isostatic pressing, self propagation high temperature synthesis (**SHS**) etc. Not all of the above techniques are used for the preparation of laminated composites to use them as end products, but requires further densification operations such as sintering and/or hot rolling. The present section of this chapter will discuss some of the above processes for making laminated composites.

2.1.1. Roll Compaction

Among all the *P/M* routes, processing involving roll compaction of metal powders is the most common and commercially attractive process for thin strip production. The roll com-

5

paction process has several variations and Dube [6] broadly classified them into the following categories.

    1.Routes based on roll compaction of,

    a)cold metal powder,

    b)bonded metal powder in the form of a coherent strip,

    c)hot metal powder.

    2.Routes based on the roll compaction of metal particles other than powder, e.g., compacted strip process.

    3.Routes based on the consolidation processing integrated with the powder production process e.g., spray rolling, direct steel process, direct strip process etc.

In the view of the multilayer composite strip preparation the *P/M* route involving roll compaction of

    a) cold metal powders i.e. direct metal powder rolling and

    b)bonded metal powder in the form of coherent strip have become attractive.

In **'DIRECT METAL POWDER ROLLING'** a coherent self-supporting green strip is produced by supplying cold metal powder into the roll gap of a specially designed powder rolling mill which is usually of 2-high type or 4-high type. The powder supply could either be horizontal or verticle, while later is preferred to avoid the difficulty of feeding loose powder into the roll gap. There exists two basic methods of feeding metal powder into the roll gap, namely saturated and unsaturated feed systems. In saturated feeding system an excess amount of powder is fed to the nip of the rolls where the frictional forces in between the powders, the powder and the rolls and the flow properties of the powder determine the total flow of the powder to the roll gap. The powder head in the hooper determines the quality of the green strip after roll compaction. In the unsaturated feeding system, a metering devise is used in the feed hooper to regulate the amount of powder being fed which generates considerable amount of control difficulties in direct powder rolling. Now a combination of the two, which is known as 'forced feeding' is usually followed to obtain acceptable strip quality.

An interesting application of direct powder rolling in making trimetllic multi-layer strip is described by Dustoor [7]. A low cost steel backed aluminium base bearing strip was prepared following direct powder rolling which consisted of preparing an aluminium base bearing layer sandwiched between two surface layers i.e. trimetallic green strip by a powder rolling technique shown in Fig. 2.1.

Bonding powder   Prealloyed bearing powder

Hopper   Hopper   Hopper

Process powder

Metering blades

+   +

Compacted bearing strip sandwiched between bonding layer and processlayer
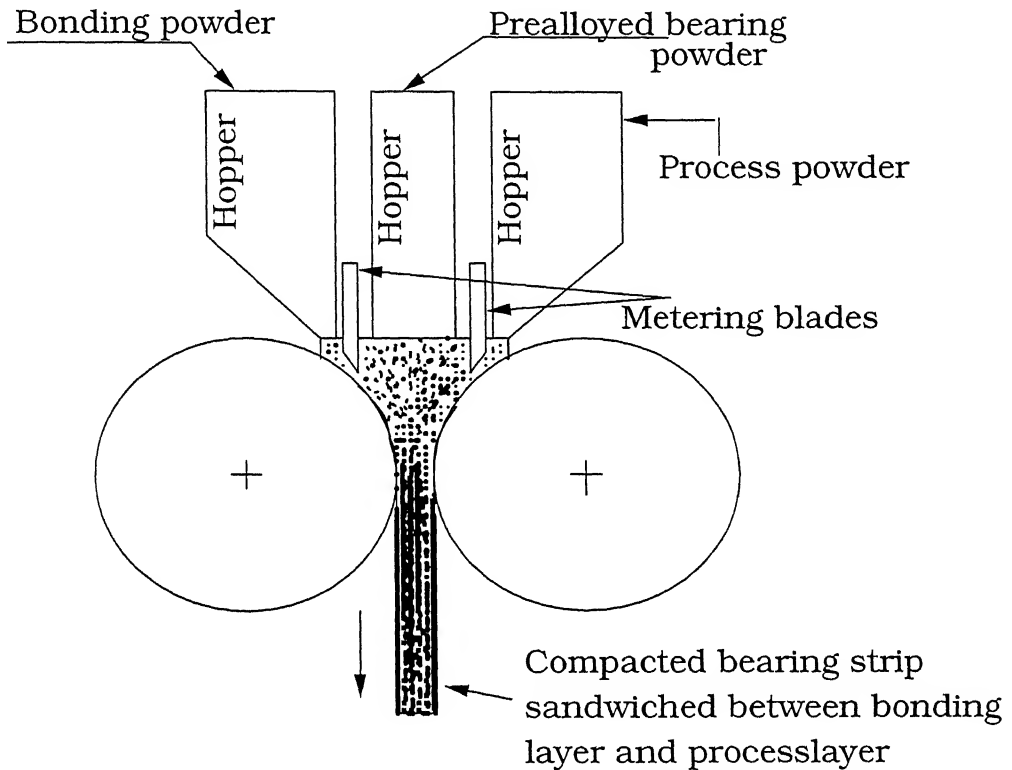
Fig 2.1:Typical arrangement for rolling trimetallic strip

The aluminium base bearing layer was made from atomized alloy powder having a composition of Al-8.5Pb-4Si-1.5Sn-1Cu, which had immiscible lead in finely dispersed state in the alloy powders. The surface layer on one side of the bearing layer was of pure aluminium powder which allows easy cladding to a mild steel strip back-up and the other surface layer was of a metal powder which acted as a sacrificial layer ('process powder') which helps in separation of the alloy strip from the rolls of the powder rolling mill. The process powder layer was machined off in subsequent bearing finishing operations. The rolling process provided sufficient shear and deformation of each powder particle due to which a strong green

7

strip resulted from the process. This was practiced by Imperial Clevite Inc., Technology centre in Cleveland, Ohio, USA. According to Ro and Toaz [8] it was possible to produce 100% dence green strip which was subsequently sintered at 813K in coil form to enhance strength and ductility of the strip. But there lies a difficulty in the form of variation in density across the thickness of the rolled green strip which could probably be attributed to the different deformation behaviours of powders of the various layers in the strip.

In a fascinating study on the rolling of trimetallic Cu-Fe-Cu green strip, Katrus and Vinogradov [9] observed that the outside copper layers became more dense than the core iron layer under the same pressure indicating different deformation behaviour of copper and iron in the trimetallic strip. Direct powder rolling is also used to produce porous nickel strips, used in alkaline battery and fuel cell electrodes, by using a spacing agent such as methyl cellulose powder in the feeding mix prior to the roll compaction [7,9].

In 'BONDED METAL POWDER ROLLING', bonded metal powder is fed into the roll gap in the form of a flexible coherent strip. This enables the feeding of accurate amount of powder into the rolling mill which is difficult to achieve in direct powder rolling technique. The preparation of green strip by this method consists of the following basic steps [6],

1. preparation of a slurry mixture from metal powder, a binder, a solvent medium and a plasticizer depending on the nature of binder,

2. deposition of the slurry on a substrate,

3. drying of the slurry on the substrate which after removal from thesubstrate yields a coherent and flexible green strip,

4.densification of dried strip by roll compaction followed by other operations like sintering, rolling, annealing etc.

Since the major importance is given to the process of the slurry preparation, this is also known as 'slurry technique' which has some similarity with the powder injection moulding (**PIM**) process in terms of the slurry chemistry and mixing operations.

The slurry is made with metal powder, binder, plasticizer and solvent medium keeping the final viscosity in the range of 1 to 1000 Poise which makes the slurry substancially homogeneous over a period of time. Thixotropic behaviour arises if too high a solids content

is used and the process is sensitive to small variations in temperature and solids content. So a slurry composition is optimized by practice keeping in mind the demands for a particular syster. Generally the constituents of a slurry are mixed slowly to avoid air bubble entrapment. To get rid of the adsorbed gases the slurry is transferred to a chamber maintained under vacuum.

After removing the adsorbed and entrapped gases through evacuation technique the mixure is poured into a mould or subtrate with the help of a doctor blade mechanism to maintain the uniformity of the slurry thickness. This doctor blade assisted slurry casting process is also known as 'tape casting' and is widely followed in industry since it is useful for continuous processing. The cast 'tape' is dried in the next step to remove the excess solvent and impart strength to the 'green' tape through gelling reaction in some water based systems. The dride tape/strip is subsequently roll compacted. Fig.2.2 schematically shows a three stage process for making laminated composite by using slurry technique.

2.1.2. Cold Isostatic Pressing

The term *'Isostatic Pressing'* is the name given to any process that applies pressure simultaneously and equally in all directions to a powder mass. If the pressure transmitting medium is a liquid, then the process is more specifically referred to as *'hydrostatic pressing'*. If other pressure transmitting media, such as rubber, plastics, powders, gases are used the broader term of *'Isostatic Pressing'* is employed [10].

Cold isostatic presses are designed either according to the wet-bag or dry-bag principle. The main difference between the two types is the tool holding systems. In the wet-bag press the tool is placed directly in the liquid in the high pressure vessel where as the tool in a dry-bag press is separated from the liquid by a pressure transmitting membrane [11]. Due to these differences wet-bag presses are normally suitable for production of a short series of complex parts where manual handling can be accepted. Dry-bag presses are suitable for mass production with a high degree of automation.

The advantage with cold isostatic pressing is the green density of the compact is higher than that after uniaxial pressing. Besides the positive effect of the isotropic stresses the possibility to press with out lubricant has a large benifitial effect on green strength. A number of factors, such as

a)more efficient transfer of pressure with in the compact,

b)elimination of die wall friction,

c)elimination or reduction of lubricant, will influence to achieve higher densities.

Metal slurry I   Glass mould

STAGE I

Metal slurry II

STAGE II   Glass mould

Metal slurry II

STAGE III   Metal slurry I

Metal slurry II

Metal slurry I
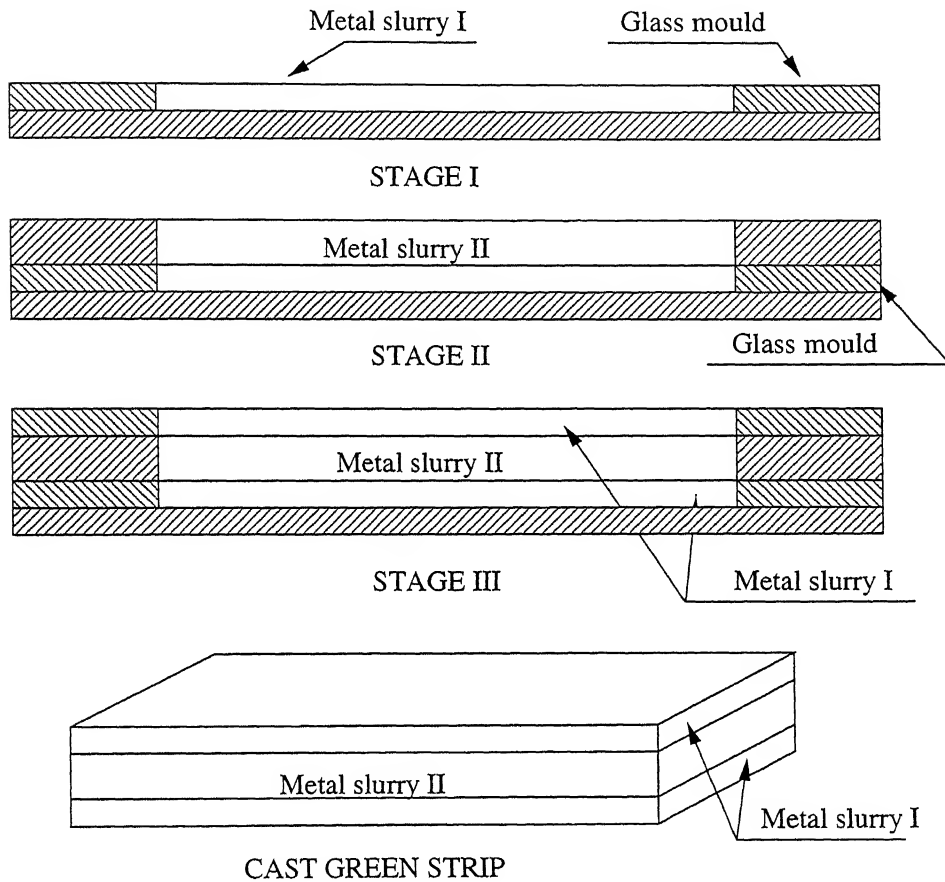
CAST GREEN STRIP

Fig 2.2 : Three stage slurry casting process

2.1.2.1 Sintering

The green strip/compact produced by the above methods require further densification operations such as sintering and/or hotrolling. Sintering is defined as "*The process by which an*

assembly of particles, compacted under pressure or simply contained in a container, chemically bond themselves into a coherent body under the influence of an elevated temperature".
The green compact containing 20-25% porosity is low in strength and ductility, which is sintered at suitable temperature to improve physical and mechanical properties. Sintered compact, due to good bonding between the particles by neckgrowth, possess significant strength and ductility and is capable of withstanding the handling involves in the subsequent operations. Sintering also removes undesirable impurities e.g. surface oxide films and sulfur from the powder mass provided a suitable sintering atmosphere is used. This atmosphere protects the green strip from oxidation which takes place on the surface as well as in the interior portions of the strip due to inter connected porosity.

Furnace atmosphere in powder metallurgy are generally classified as oxidizing, reducing, carburizing and inert [12]. Generally a reducing atmosphere of either dry H_2 or cracked NH_3 is provided during sintering for a large number of systems. Inert gas atmospheres like N_2 and argon are another popular choice because of their non reactive nature. Some times sintering in vaccume is also carried out as it is clean, reproducible and relatively easy to control. This helps to avoid a low partial pressure of oxygen which can lead to oxide reduction for many metals.

2.1.2.2. Post-Densification Techniques

The strip/compact obtained after sintering is quite porous though some amount of densification occurs in sintering which gets reflected in the improved strength and ductility properties of the strip. To achieve full density in the strip they are subjected to post-sintering densification processes which can be classified into two broad categories [6].

      a)repeated cold rolling and sintering/annealing cycle and

      b)hot rolling.

(a)Repeated cold rolling - sintering/annealing cycle
Many investigators have reported of obtaining fully dense metal strips made from roll compacted and sintered powder preform by a series of cold rolling and sintering/annealing cycles [13-16]. The porosity content in the sintered preform determines the amount of cold

rolling required for full densification of the strip. It is reported that this field lacks in extensive systematic studies for detailed understanding of the mechanism involved in full densification. Hunt and Eborall [13] showed the dependence of the amount cold rolling reduction between each anneal in a copper system on the initial density achieved in the preceding anneal, the variation of the density across the strip width and weather or not the strip is coiled after rolling. Sturgeon et al. [14] studied the effect of cold rolling on the mechanical properties of sintered stainless steel strips which revealed an optimum peak tensile strength with the amount of cold reduction beyond which mechanical properties deteriorated probably due to fragmentation of inclusions caused by microcracks at the inclusion-matrix interface.

This process route suffers from the disadvantage that it requires several cold rolling and annealing cycles to produce full density strip which impaires its commercial viability.

b)Hot Rolling

Many investigators have proposed hot rolling after sintering as a means of achieving full density in metal strip. Sintered strip having porosity content as high as 80% can be hot rolled to full density in a single pass [6,17]. The advantage offered by this process are that it enables to produce full density strip in a single operation while reducing the sintering time and it is possible to hot roll the sintered strip/compact from the sintering furnace directly after sintering, thereby saving time and energy and offering the possibility of continuous processing. The amount of hot rolling reduction, required to achieve full density in the final strip is dependent on the initial porosity of the strip and it is greater than the theoretically required reduction since some amount of rolling deformation goes in elongating strip instead of closing the pores. The densification in this process results from compaction by rearrangement and restacking of particles in the systems under the specified conditions.

2.1.2.3 Final Cold Rolling and Annealing

The P/M strips produced through the hot rolling route are sometimes given a certain amount of cold reduction and annealed before despatch, while the strips produced through the repeated cold rolling and sintering/annealing cycle route are invariably given a final annealing treatment according to the requirement before despatch. This is done to achieve better surface property along with better and homogeneous overall strip properties.

12

2.1.3 Hot Pressing and Hot Isostatic Pressing

These techniques refer to a process in which an external pressure is applied to the powder compact while heating. These methods are also known as pressure sintering or pressure assisted sintering [18]. The main difference between these two processes is the method in which the pressure is applied. In hotpressing, pressure is applied uniaxially to the powder in a die, whereas in hot isostatic pressing, the pressure is applied isostatically by means of a gas. Of the two methods, hot pressing is simpler and more widely used. However, the use of hot isostatic pressing has been increased in recent years. Hot pressing and hot isostatic pressing have similar capabilities in terms of the temperature that can be used. Depending on the type of furnace, temperatures as high as 2750K can be used with many types of commercial equipment. However because of the different ways in which the pressure is applied to the sample, clear difference exists between the two methods in terms of the pressure capability and ease of fabrication.

In *'Hot Pressing'*, the powder or a consolidated powder is placed in a die and heated while pressure is applied. Depending on the furnace, operating temperatures of upto 2750K can be used. Typical operating pressure range from 10 to 75 MPa. The maximum applied pressure is essentially limited by the strength of the die. Pressures upto 40 MPa are typical for the commonly used graphite dies. The use of speciality graphite and more expensive refractory metal (e.g., nimonic alloy) or ceramic (e.g., Al_2O_3 and SiC) dies increases the maximum pressure to 75 MPa. Graphite oxidizes slowly below 1475K, so it can be exposed to an oxidizing atmosphere for short periods. Above 1475K, it must be used in an inert or reducing atmospheres. Only discs and simple shapes can be produced by hot pressing.

In hot isostatic pressing, commonly abbreviated **HIP**, the sample is placed in a pressure vessel, the gas pressure is applied, and the temperature is raised. Achieving the required pressure at firing temperature relies on heat-up of the gas by the HIP furnace. Pressures upto 200 MPa are routinely available in most equipment. Samples with a continuous network of open porosity, in HIP, must be encapsulated within a sealed metal or glass can that provides a medium for transmitting the pressure to the sample. Without the can, the pressurized gas enters the pores and resists the compressive sintering stress so that only highly porous materials are produced. HIP allows fairly complex shapes to be fabricated.

2.1.4 SHS Method

Once initiated, highly exothermic reactions can become self-sustaining and will propagate through the reactant mixtures in the form of a combustion wave. As the combustion wave front advances, the reactants are converted to the products. The use of such reactions to prepare materials have been commonly referred to as *self propagating, high temperature synthesis* (**SHS**) method.

Numerous investigations [19-22] have been made on the preparation of intermetallic compounds and metal-intermetallic layer sheet composites by the SHS method. The aluminide systems investigated under this method include Nickel [20,21], iron [22], copper, molybdenum, titanium and zirconium. Because of relatively low heats of formation of many intermetallic compounds, they are commonly prepared by the 'thermal explosion' mode of SHS, in which the reactant mixture is heated in a furnace at a constant heating rate until the combustion reaction takes place spontaneously. Recent investigations on the Al-Ni system have shown that the combustion reaction is influenced by precombustion phase formation driven by solid state diffusion [21]. It has been demonstrated that the extent of formation of these precombustion phases can influence the mechanism of combustion and consequently, the characteristics of product. The attractiveness of the SHS as a process for the synthesis of materials stems from a variety of considerations. The most important of these include the energy savings associated with the use of self-sustaining reactions, the simplicity of the process, the relative purity of the products, and the possibility of simultaneous formation and densification of the product. Additionally, in some cases it has been demonstrated that the products developed by the SHS process are superior to those prepared by conventional means. Another advantage of SHS process is its suitability for the preparation of solid solutions, composites and metastable phases.

2.2 Intermetallic Compounds and their Importance

For many years, the beneficial effects of long range order on strength, especially at elevated temperatures, has created a lot of interest in possible applications of intermetallic compounds. Intermetallic compounds can be defined as intermediate phases in an alloy system having a narrow range of homogeneity and relatively simple stoichiometric proportions. In

14

these compounds, the nature of atomic bonding can vary from metallic to ionic. These compounds have recently emerged as the potential high temperature oxidation resistant materials for many next generation applications.

Amongst intermetallics, maximum attention has been given to aluminides of nickel, iron and titanium. The aluminides have low density because of the presence of aluminum which also provides protection at elevated temperatures by forming a protective film of alumina. Some of the important properties of the aluminides are their low density, high strength which even improves with temperature, good corrosion and oxidation resistance, relatively low cost and use of non-strategic elements. These attributes make these compounds ideal choice for several high temperature applications. Properties of some of the important aluminides are shown in Table-2.1.

TABLE 2.1 Important Aluminides and Their Relevent Properties

Alloy	Crystal Structure	Melting Point (K)	Density g/cc	Yeild Strength (MPa)	Young's Modulus $(\times 10^3 MPa)$
Ni_3Al	LI_2 (Ordered *fcc*)	1663	7.5	250 - 500	178.6
NiAl	B_2 (Ordered *bcc*)	1913	5.9	250 -475	294.4
Fe_3Al	DO_3 (Ordered *bcc*)	1813	6.7	385 - 475	140.7
FeAl	B_2 (Ordered *bcc*)	1523	5.6	360 - 380	260.6
Ti_3Al	DO_{19} (Ordered *hcp*)	1873	4.2	700 - 900	144.8
TiAl	LI_0 (ordered *tetragonal*)	1733	3.9	400 - 650	175.8

The major disadvantage of most of the intermetallic alloys is their low ductility and toughness. The long range ordering which provides these intermetallics high strength also makes them extremely brittle in certain systems at low temperatures. Alloying additions,

both at macro level (e.g., Nb in Ti_3Al) and microlevel (e.g. B in Fe_3Al and Ni_3Al) have been successful to an extent in reducing the problems of poor ductility and toughness. Control of microstructure is another approach taken for ductilizing these materials. Currently, titanium aluminides are candidate materials for aerospace applications, nickel aluminides for applications as long life heating elements and forging die materials and iron aluminides for coal gas environment techniques.

2.3 Iron Aluminide

2.3.1 The Fe - Al System

Iron aluminides have been of interest since 1930's when their excellent oxidation resistance was first noted [23, 24]. Since the observation of Bradlay and Jay, research has continued on these materials to improve their room temperature ductility and strength above 873K. All of these studies have resulted in significant contributions to the fabrication and mechanical properties of iron aluminides. A number of investigations have been done regarding the mechanical behavior of Fe_3Al (like ductility, strength, temperature dependence of the deformation, crack, fatigue etc.) and also lot much efforts are being made in improving their mechanical behavior in order to make these alloys suitable for practical purpose.

2.3.2 Crystal Structure

The Fe-Al system is characterized by a wide α-Fe solid solution range upto about 18at% aluminum at room temperature. However, with increasing aluminum content various stable phases occur, namely Fe_3Al, $FeAl$, $FeAl_2$, Fe_2Al_3, $FeAl_3$ and each of this has a homogeneity range (Fig.2.3) [25,26]. Out of these, there are two ordered phases of interest which have DO_3 and B2 ordered super lattice structures (Fig.2.4 and Fig.2.5). These two ordered structures with stoichiometric compositions Fe_3Al and $FeAl$ can form the disordered bcc α-phase in Fe-Al alloys. These structure can exist over a wide range of compositions. At equilibrium, Fe_3Al occurs as a DO_3 structure between 18.5 and 36.5 at% Al at room temperature while FeAl in B2 structure, exists between 36.5 and 50at% Al [27]. In a certain composition range, the direct transition from Fe_3Al to FeAl type order is possible. The DO_3 structure
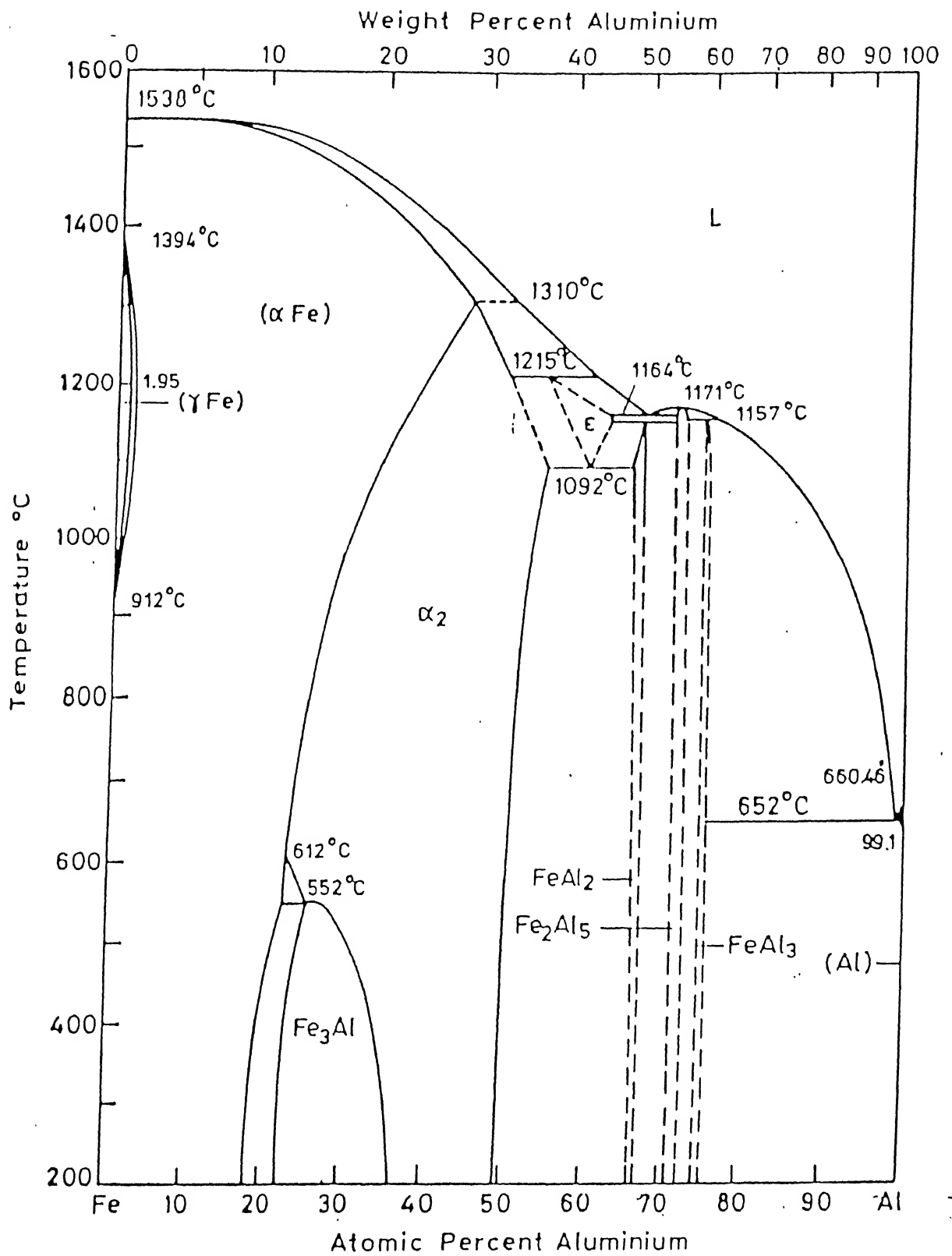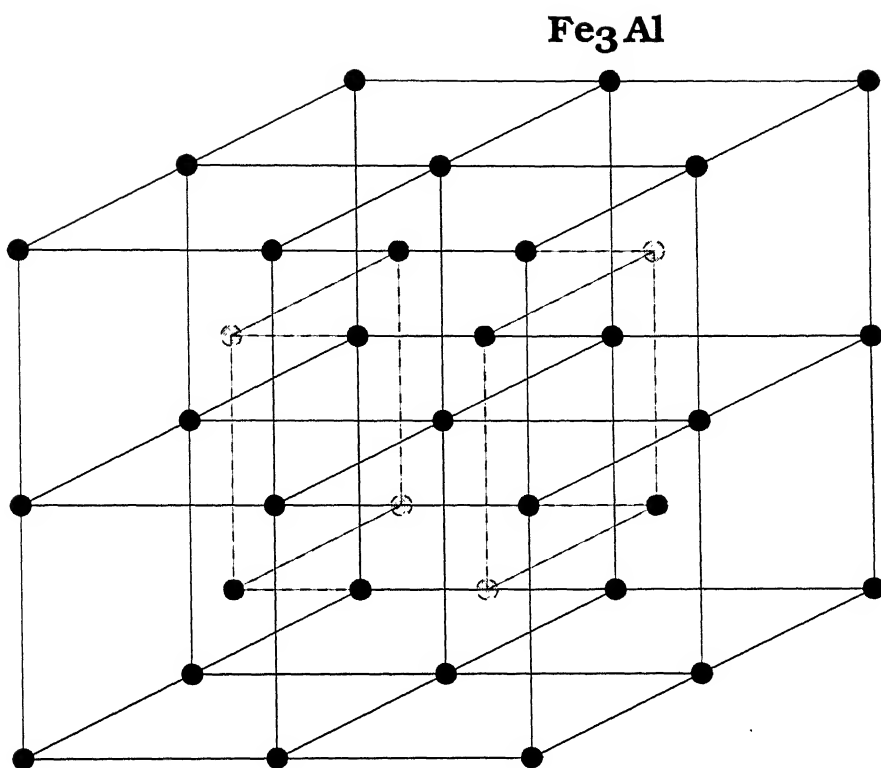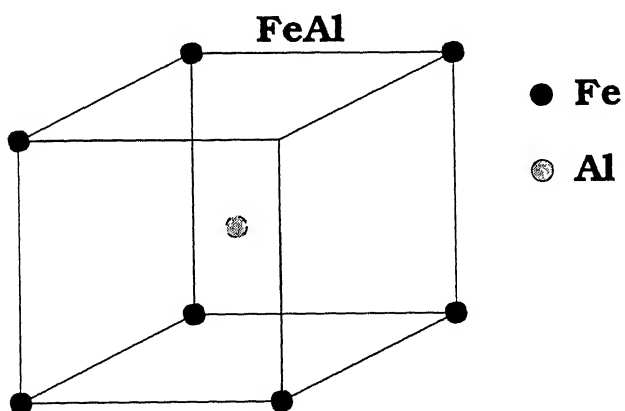
Fig.2.3 : Fe -Al binary phase diagram

17

Fe$_3$Al

Fig 2.4

DO$_3$ Crystal structure

FeAl

● **Fe**

◉ **Al**

Fig 2.5

B2 Crystal Structure

stable only upto 813K. Above 813K, the B2 structure is stable.

The ordered DO_3 structure consists of eight bcc cells with each unit cell consists of a total of sixteen atoms. Four atoms are of Al at $(3/4, 3/4, 3/4)$, $(3/4, 1/4, 1/4)$, $(1/4, 3/4, 1/4)$, $(1/4, 1/4, 3/4)$ lattice sites and the remaining sites are occupied by twelve Fe atoms. Although the disordered lattice is bcc, the ordered has a symmetry as fcc structure owing to tetrahedral arrangement of Al atoms. The B2 structure have two interpenetrating simple cubic sublattices with the atoms of each constituent at the body center of the other. It consists of Fe atoms at $(0, 0, 0)$ and Al atoms at $(1/2, 1/2, 1/2)$ lattice sites. Studies of phase relationships in Fe-Al systems have confirmed [28] the following equilibrium phases near the Fe_3Al composition: a disordered solid solution(α), Fe_3Al with an imperfectly ordered B2 structure, and ordered Fe_3Al with DO_3 structure, the two phase regions of α+DO_3 and α+B2.

2.3.3 Mechanical Properties of Iron Aluminides

2.3.3.1 Ordered DO_3 Fe_3Al-based Aluminides

There has been extensive work on the study of mechanical properties of iron aluminides based on Fe_3Al. An early work of Justusson et al. [29] on alloys containing 15-28 at% Al shows maximum strength and minimum ductility near the stoichiometric Fe_3Al composition. It was found that there is a transition in yield strength from 470 MPa at 27 at% Al to 720 MPa at 26 at% Al, and further increases as the aluminum content goes down to 24 at% Al. The transition from high yield stress value for 26 at% Al to a lower yield stress value for 27 at% Al corresponds to the boundary between α+DO_3 phase fields at 773K. Based on this, Innoune et al. [30] have shown that the higher ambient strength of 24-25 at% Al compositions is because of age-hardening effect of α precipitated in DO_3 phase during the ordering treatment at 773K. The high yield stress of lower Al content alloy is caused by a low mobility of dislocations coupled closely with **APB**'s (Antiphase boundary). Above 26 at% Al, the APB energy of <111> fault vector increases substantially and deformation is, therefore, by highly coupled superlattic dislocations. The ductility increases from 1% at 24 at% Al to 5% at 30 at% Al is apparently associated with a drop in yield stress resulting from increasing Al content. Temperature plays a major role on the mechanical properties of Fe_3Al based aluminides [31]. Here the behavior of various compositions can be grouped

into two regions namely upto 24 at% Al and another group from 28-30 at% Al composition range. As explained earlier, the higher ambient strength of 24 at% Al composition is attributed to presence of α precipitates in DO_3 matrix producing age hardening effect. The composition range 28-30 at% Al is in DO_3 phase field and these exhibit the anomalous strength peak at approximately 823K which corresponds to the second order transformation temperature from DO_3 to B2. This type of yield behaviour has been observed in many other ordered systems including Ni_3Al, CuZn [32], Ni_3Mn and FeCo. In Fe_3Al alloys, the peak strength has been related to a critical degree of long range order [33,34]. The value of the long range parameter S is shown to be 0.8 at room temperature and drops to 0 beyond the B2 transformation temperature. The critical order parameters are shown by Hanada et al. [34] to lie in the range of 0.5-0.6 at the strength peak temperature irrespective of the DO_3 to B2 transformation temperature have been successful in improving the strength levels upto 1073K [35,36]. Alloying of Fe_3Al with various elements (less than 10 at%) could produce improvement in properties. Addition of 2 at% Cr improves the ductility from 3.7% to 9.4% with adversely affecting the room temperature and elevated temperature strengths. Chromium addition enhances the fracture strength for transgranular cleavage to a level comparable to that for intergranular fracture. This produces an increase in elongation before the onset of failure. Flow stress may reach both cleavage and interfracture strength. Alloy addition reduces brittle cleavage fracture through enhancement of cleavage strength. Chen et al. [37] has reported improvement in creep properties by alloying with Cr, Zr and B. Rupture life of 222 hours as compared to 1.6 hours for unalloyed Fe_3Al and percentage creep elongation 14.8 as compared to 33.6 (tested at 200 MPa, 873K). Another major area of study in Fe_3Al intermetallics is the environmental effect. Fe_3Al is highly environment sensitive alloy. Environmental effects on room temperature ductility and fracture in Fe_3Al has been studied by many authors [38,39,40]. Their result show that Fe_3Al is less prone to embrittlement as compared FeAl because of lower Al content. But still it is susceptible to environmental embrittlement at ambient temperatures in the presence of water vapour. High ductility of above 12% has been obtained in Fe_3Al when tested in vacuum or dry oxygen environment. The embrittlement involves the reaction of water vapor with Al atoms and the release of embrittling atomic hydrogen which is absorbed by the specimen leading to reduction in ductility. The Fe_3Al alloy always showed cleavage and their fracture mode doesn't change with test environment.

2.3.3.2 Ordered B2 FeAl-based Aluminides

The room temperature ductility and toughness of FeAl based aluminides has been reported to be poor [38,39]. The Fe 31 at% Al(DO$_3$) exhibited a room temperature ductility of about 5.6% which decreased to 2.5% for Fe-40 at% Al and a premature totally brittle failure was observed in Fe-50 at% Al alloy. Alloys with some ductility failed in transgranular cleavage mode. While Fe-50 at% Al with nil ductility exhibited intergranular fracture. Therefore, with increasing Al in the FeAl (B2) regime of the phase diagram the ductility at room temperature decreases rapidly. However, the positive factor is their reasonable strength retention (upto 40 at% Al) to 873K (Y.S. ~414 MPa). This is in contrast to the yield strength drop of Fe$_3$Al aluminides at around 823K near DO3→B2 transition. Mendiratta et al. [41] have studied the basic dislocation mechanism for B2 FeAl alloys containing 35 to 50 at% Al, and reported that binary FeAl deforms by ⟨111⟩ slip at low temperatures and ⟨100⟩ slip at high temperatures. The same has been observed by several other workers [42,43]. This means a reduction from five to only three independent slip systems which are insufficient for uniform plastic flow in a polycrystalline. The transition temperature for ⟨111⟩ to ⟨100⟩ slip was found to be composition dependent. The transition temperature was found to be about 623K for 50 at% Al and increased with decreasing aluminum content, being about 698K for 40 at% Al composition. Baker et al. [44] have shown that for Fe-40 at% Al composition deformation is mainly by ⟨111⟩ slip upto 698K and ductility increases with increasing temperature presumably due to ease of cross-slip. Above 698K slip occurs mainly by ⟨100⟩ dislocations. Ductility was possible at 798K due to the presence of few ⟨111⟩ dislocations and, at still higher temperatures (where no ⟨111⟩ dislocations were found) due to the occurance of diffusion assisted processes. Above 898K, a ductility drop occurs accompanied by a change in fracture mode from transgranular cleavage to intergranular cavitation. This is due to grain boundary weakening taking place because of equicohesive temperature effect [44]. The alloying additions such as Zr and Hf will increase the strength of Fe-40 at% Al, but all ternary additions reduces the ductility except that B, C and/or Zr containing alloys showed the ductility to be about 5% [45].

21

2.4 Processing Routs for Aluminides

Many possible routes for the production of iron aluminides is shown in Fig.2.6 [46]. Among these the melting route is the most economical. However, the selection of melting route for iron aluminides is associated with many issues. The use of wet charge or moisture around the melting crucible can result in the generation of large amount of hydrogen. The molten iron aluminide dissolves this hydrogen, which cannot escape during solidification and produces large voids. The selection of suitable crucible for the melting of iron aluminide is also important inorder to minimize the impurity pickup from the crucible material.

2.4.1 Powder Metallurgical Processing

The problems associated with melting and casting of large ingots can be greatly reduced by using powder metallurgical routes.

2.4.1.1 P/M Route Based on Prealloyed Powder

The prealloyed powders of refined composition are produced using the usual powder production methods such as atomization. The powders so obtained can be subjected to thermo mechanical processing in order to obtain dense, monolithic near net shape components with appropriate microstructures. At present, the availability of prealloyed iron aluminide is also limited and due to their low diffusivity, high strength and brittle nature, the consolidation becomes even more difficult. This results in a high degree of porosity and inhomogeneity in the composition.

2.4.1.2 P/M Route Based on Elemental Powder : Mechanical Alloying

This route by passes the difficulty incurred during the handling of molten metallic solution to produce the prealloyed powder. The process utilizes either the elemental or certain master alloy powders which are readily available and inexpensive [27]. In mechanical alloying blending is caused by compressive forces generated in the powder particles trapped between the colliding balls. Each collision involved cold welding of particles, a reduction of thickness of each phase and introduction of dislocation into the powder composite particles. Once the limit of cold work (a dislocation density of 1×10^{16}/sq.m.) is reached in the welded
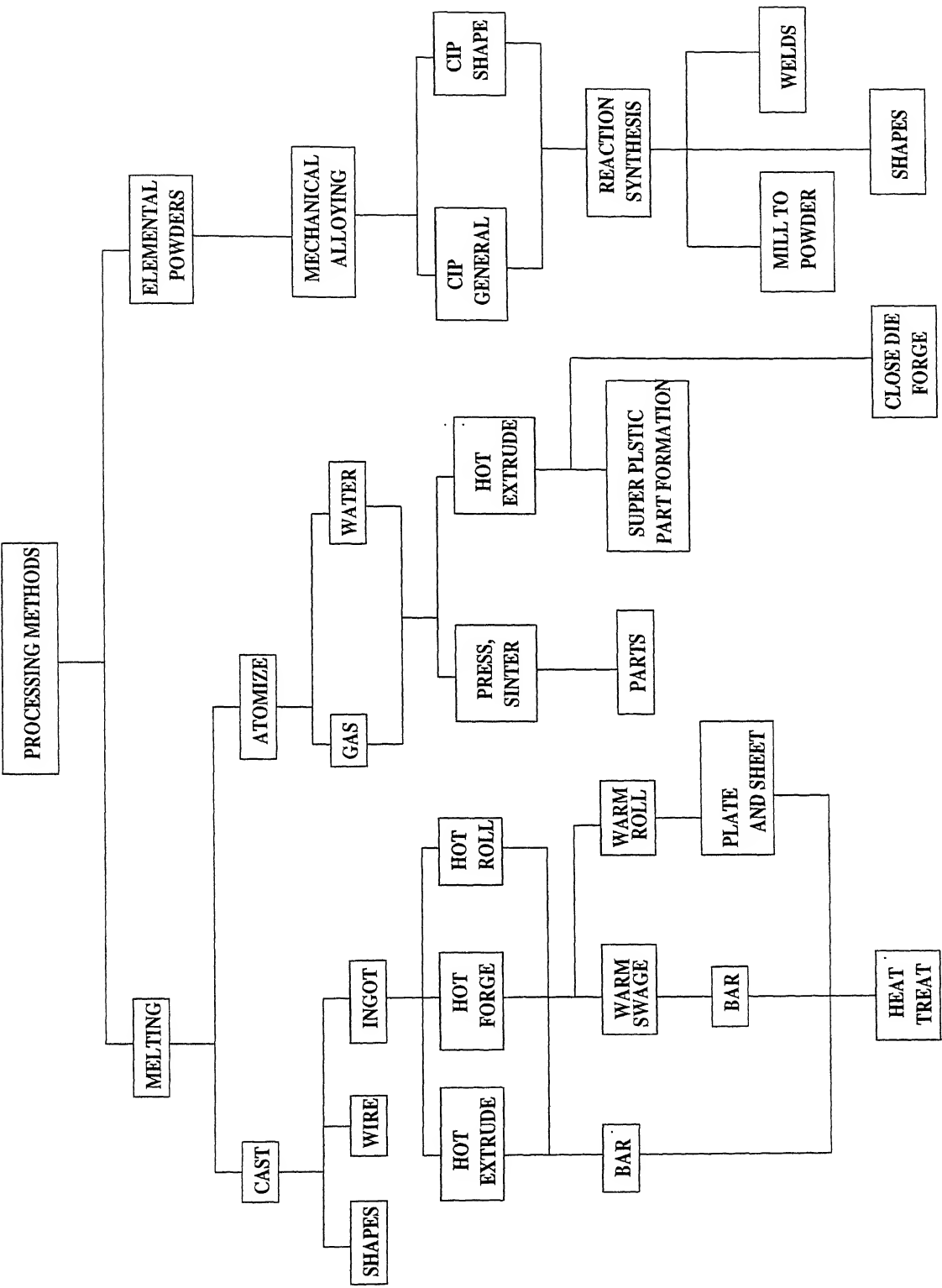
22

Fig.2.6 : Possible Routes for Iron Aluminide Production

23

composite particle, fracture occurs [47]. Through repetitive cold welding fracture cycles, a dividing and kneading process is established which finally leads to alloying on an atomic level. A large number of dislocations are introduced into the powders during mechanical alloying which enhances the diffusional process. For ductile materials, this process is easily possible, but the high strength brittle materials like aluminides it may require very high energy milling to generate extremely high dislocation density to cause enhanced diffusion.

2.5 Metal - Intermetallic Laminated Composites

Metal-Intermetallic composites are unique structures, as they offer an attractive combination of properties from both component phases, i.e. high stiffness, high modulus and low density of the intermetallic and high toughness of the metal. Previously, intermetallic matrices have been reinforced with ductile metals in the form of particles, fibers, tubes and layers. These composites have been fabricated via traditional solidification techniques, pressure-aided consolidation of prealloyed intermetallic powders mixed with the ductile reinforcement. Recently, metal-intermetallic layered composites were formed by using self-propagating, high temperature synthesis(**SHS**) method [22,48,49], in which alternative layers of aluminum and metal foils were stacked together and were heated. After the reaction, one of the metal foils was entirely consumed, resulting in a metal-intermetallic laminar composite. In a study by Alman et al. [22], five layers of aluminum foils (each 0.15mm thick) were alternately stacked between six layers of metal foil (Ni, Ti or Fe, each 0.15mm thick). The foil sandwiches were placed between the cylindrical graphite platens of an induction heated vacuum hot press. The stacked foils were heated to 873K and held for 60 minutes with no pressure applied on the composites other than the weight of graphite platens. The samples were then heated to 993K, which is above the melting temperature of Al. The purpose of the initial portion of the processing cycle was to initiate an SHS reaction between the elemental metal foils. The tensile properties of some of metal-intermetallic laminated composites are shown in Table 2.2.

24

TABLE 2.2 Tensile Properties Of Metal-Intermetallic Layered Composites

Composite	Fe-Al	Ni-Al	Ti-Al
YS(MPa)	169	109	102
	190	113	104
UTS(MPa)	296	256	159
	312	193	173
% E	3.9	12.0	3.2
	4.3	6.0	3.2

The composites exhibited three distinct mechanical behaviour differences:

1. lower strength and ductility displayed by the Ti-Al composite,

2. higher strength and lower ductility displayed by the Fe-Al composites,

3. higher strength and higher ductility, displayed by the Ni-Al composites.

The mechanical behavior of the composite showed some correlation with the corresponding failure mechanism. The metal layers in the Ni-Al composite exhibited extensive deformation prior to failure, with the metal layers bridging multiple cracks in the intermetallic layers. This failure mechanism was accompanied by extensive cracking of the intermetallic layer both parallel and perpendicular to the metal layers [50]. The higher strength, lower ductility composites (i.e. Fe-Al) was characterized by numerous cracks in the intermetallic layer, which formed perpendicular and parallel to the metal layers. However, some cracks propagating perpendicular to the metal layer had penetrated into the Fe layer. The penetration of cracks into the metal layer reduces the effective thickness and load-carrying capability of the metal layer, thus contributin g to the low d uctility behavior of the composite.

Chapter 3

SCOPE OF THE PRESENT WORK

The present study consists of preparing Fe_3Al-Fe-Fe_3Al and Cu-Fe-Cu laminated composite strips by a powder metallurgical route involving hot pressing of individual powder layers into a composite compact following densification rolling .

The physical and mechanical properties together with the microstructure of the laminated composite strips are also studied.

Chapter 4

EXPERIMENTAL PROCEDURE

4.1 Materials

4.1.1 Iron Powder

Electrolytic iron powder supplied by Sudhakar Products, Bombay was used. The particle size distribution of the iron powder is shown in Table-4.1 and in Fig.4.1. A typical SEM micrograph of the iron powder is shown in Fig.4.2 .

Table 4.1 : Particle Size Distribution of Iron Powder

B.S.Sieve Number	wt%
+52	0.20
+100	0.27
+200	46.20
+300	27.31
+400	11.30
+Pan	14.72

4.1.2 Aluminum Powder

Gas atomized aluminum powder supplied by Alcan Metal Powder, New jersey, U.S.A (now named as ACu Powder Ltd.) was used. The particle size distribution of the aluminum powder is shown in Table-4.2 and in Fig.4.3. A typical SEM micrograph of the aluminum
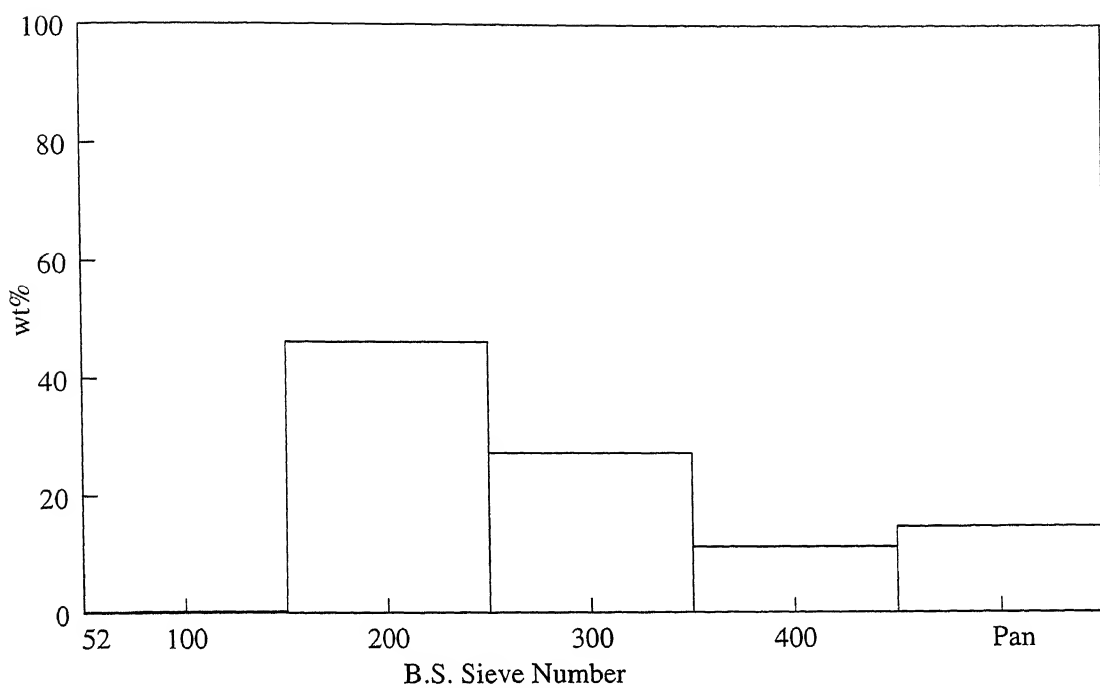
27

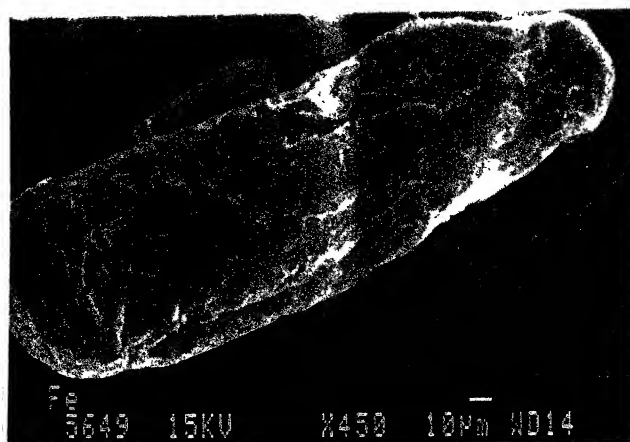Fig.4.1 : Particle size distribution of iron powder

Fig.4.2 : SEM photomicrograph of iron powder

28

powder is shown in Fig.4.4.

Table 4.2 : Particle Size Distribution of Aluminum Powder

B.S.Sieve Number	wt%
+52	2.10
+100	23.60
+200	36.16
+300	17.62
+400	11.64
+Pan	8.88

4.1.3 Copper Powder

Atomized copper powder supplied by Green back Industries, Inc., U.S.A was used. The particle size distribution of the copper powder is shown in Table-4.3 and in Fig.4.5. A typical SEM micrograph of the copper powder is shown in Fig.4.6.

Table 4.3 : Particle Size Distribution of Copper Powder

B.S.Sieve Number	wt%
+52	0.20
+100	0.36
+200	2.96
+300	9.85
+400	19.88
+Pan	66.74

4.1.4 Gases

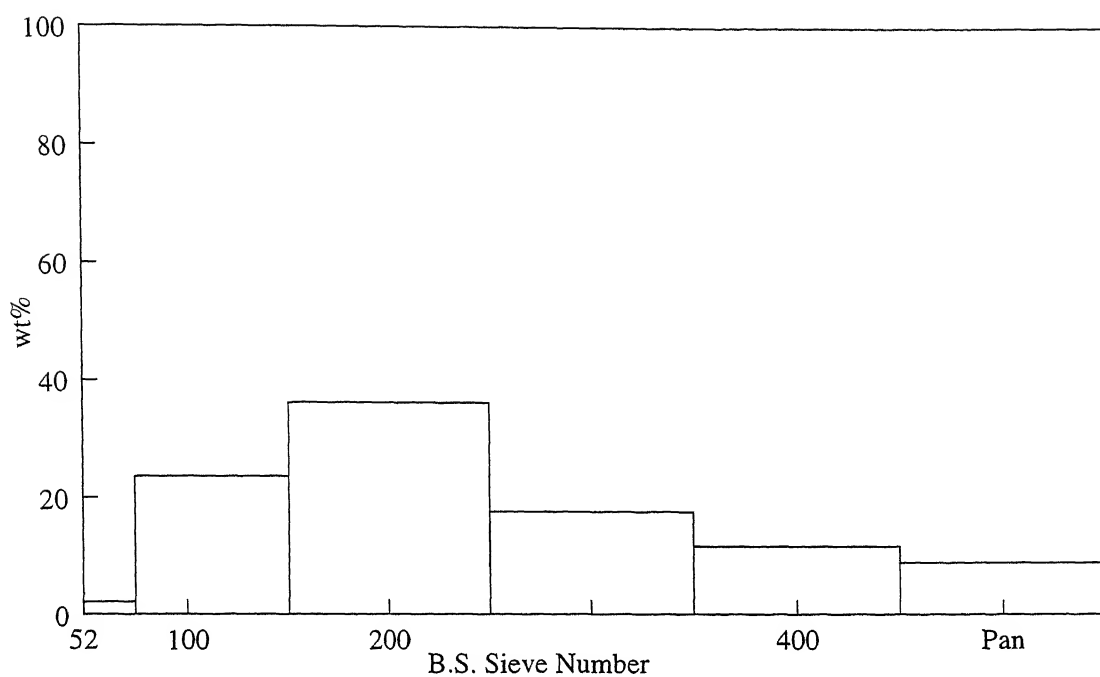IOLAR-2 grade Argon, Nitrogen and Hydrogen gases were used in the present work.
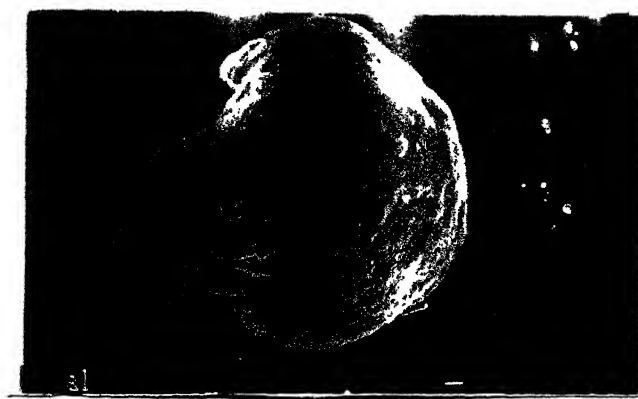
Fig.4.3 : Particle size distribution of aluminum powder

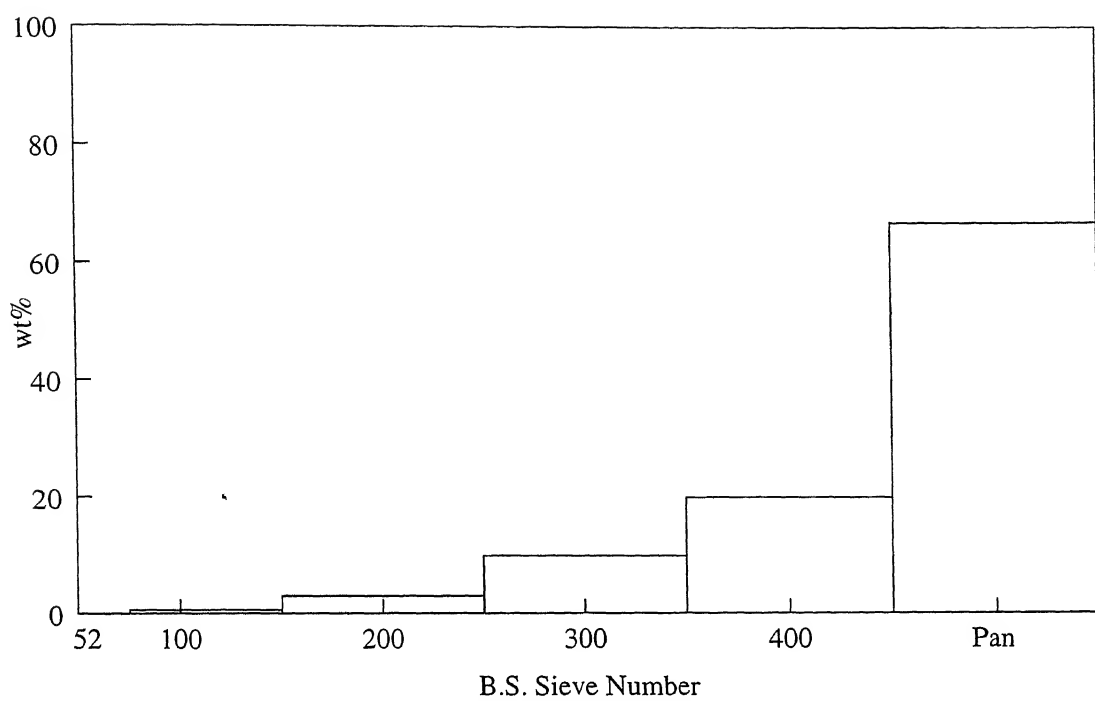Fig.4.4 : SEM photomicrograph of aluminum powder

30

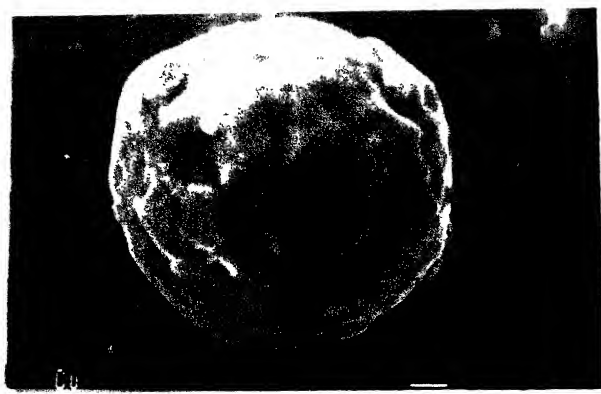Fig.4.5 : Particle size distribution of copper powder

Fig.4.6 : SEM photomicrograph of copper powder

31

4.2 Preparation of Iron Aluminide Powder

The Iron aluminide powder was prepared by mechanical alloying of high purity iron and aluminum powder in a high energy planetry ball mill manufactured by Fristch, Germany. The composition of the starting Fe-Al powder mixture was corresponds to Fe_3Al powder, which contains 86.05 wt% Fe and 13.95 wt% Al . Tungsten carbide balls of 30 mm diameter was used as the grinding media, and a ball to powder ratio of 6:1 by weight was employed. The grinding was carried out in acetone, for 24 hours, in order to prevent the excessive heating and fusing of the particles.

4.3 Preparation of the Laminated Compact by Hot Pressing

The Fe_3Al-Fe-Fe_3Al and Cu-Fe-Cu laminated composite compacts w ere prepared by using a hot press, manufactured by The Electrofuel Manufacturing Co .Ltd., Canada. The maximum temperature and load capacity of the press was 2273K and 10 ton respectively. The press assembly consists of a precision post- and-platen press, a hydraulic cylinder, and air powered hydraulic system with electrical controls . The moving water cooled ram was accurately set perpendicular to the upper platen face, while the lower stationary water-cooled base was set parallel to the lower platen face. The hydraulic system was powered by compressed air. The required hydraulic pressure was set by using a pressure regulator mounted in the control panel. As the air motor cycles, the hydraulic pressure fluctuates slightly around the set pressure. These slight periodic pressure variations have been found to be very effective in promoting densification in many cases. The modular heating unit uses molybdenum disilicide (Super Kanthal 33+) as heating elements and rests on the power connection legs. The heating unit is powered by an SCR power controller, through a step down transformer. The programmable temperature controller compares the measured temperature (from the optical pyrometer or thermocouple) to the programmed set point and request the correct power level from the SCR power controller. With the optical pyrometer temperatures can be controlled in the range of 1073K to 2273K. The thermocouple, a Chromel-Alumel type, is used to measure and control the temperature below 1473K.

A graphite die of 25.4 mm (~1 inch) inner diameter was specially prepared for making these compacts. After cleaning the die and punches, in case of Fe_3Al-Fe-Fe_3Al compacts,

first a layer of Fe₃Al powder was poured in the die and was made uniform by applying the pressure with hand on the upper punch. Uniform filling will give more uniform finished parts. In the similar way Fe powder and another layer of Fe₃Al powder on the Fe layer was poured. The filled die was then introduced in to the furnace of the hot press and was positioned under the hydraulic ram. A schematic diagram of this is shown in Fig.4.7. The same process was also employed in case of Cu-Fe-Cu compacts. In case of Fe₃Al-Fe-Fe₃Al compacts, hot pressing was carried out at a temperature of 1223K and at a load of 1 ton, where as for Cu-Fe-Cu compacts the temperature was 1173K and load was 1 ton. The only variable selected in the process of hot pressing was time. The samples of the above two systems were prepared at a soaking time of 30 min. 60 min. and 120 min.
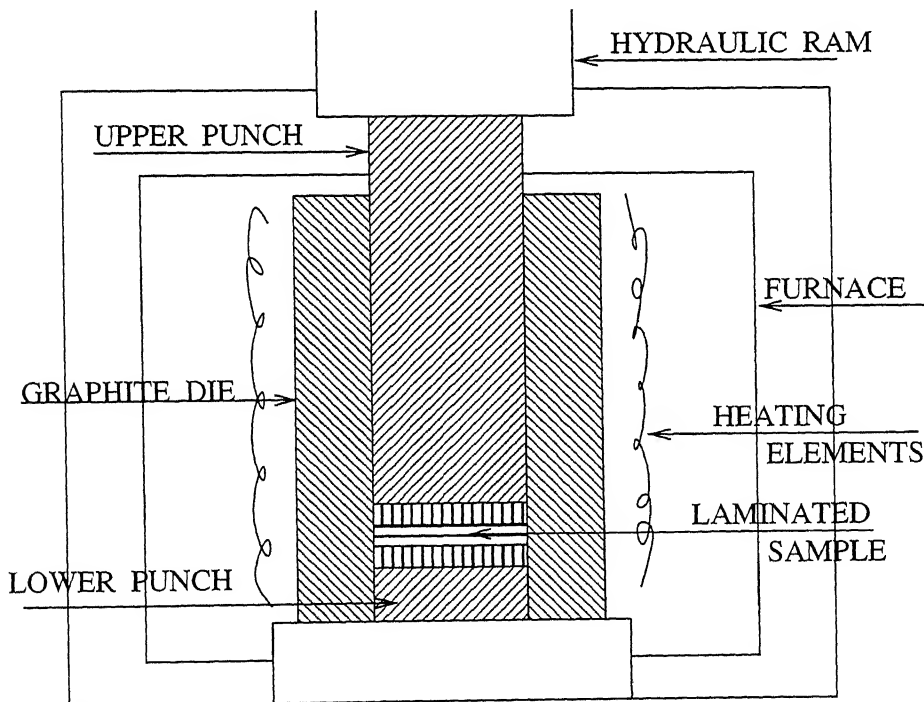
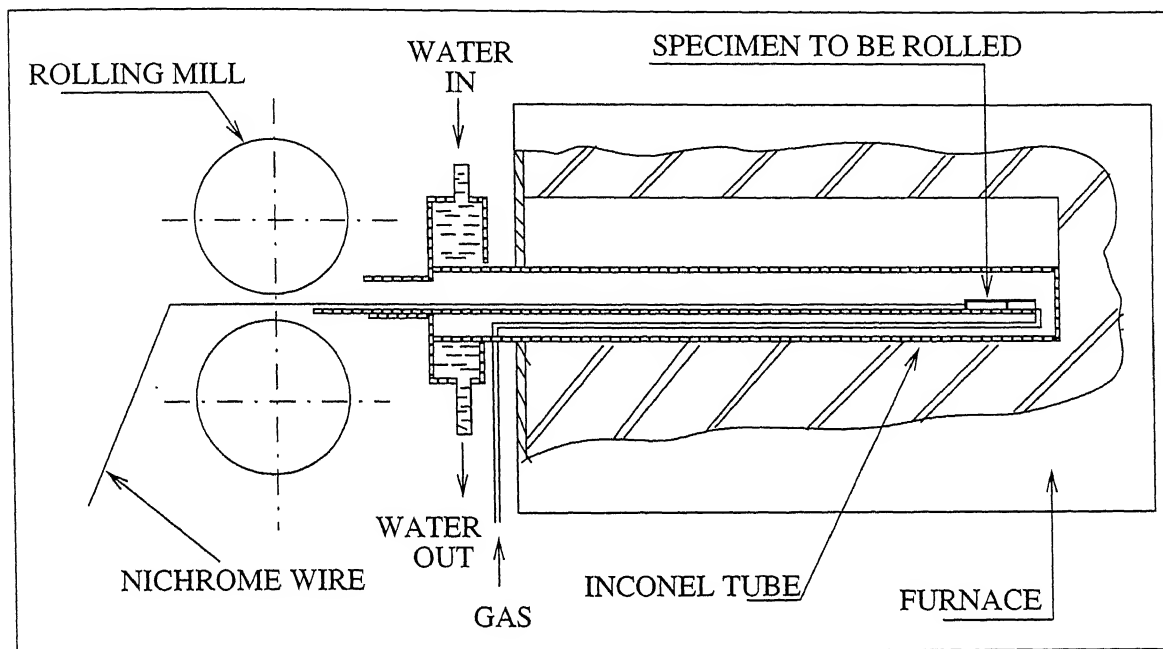**Fig.4.7 : HOT PRESSING ARRANGEMENT**

4.4 Hot densification Rolling of Hot Pressed Laminated Compacts.

The laminated compacts that were hot pressed for 120 min. were further densified by hot rolling, in order to prepare the laminated strips. A small hole was drilled near one end of the compact through which a thin nichrome wire was fastened which was required for pulling the hot compact through the rotating rolls during hot rolling operation. The compacts fastened with a nichrome wire were slowly introduced one at a time into the hot zone of a specially designed reheating furnace interlinked with a 2-high rolling mill. Hot rolling was done on a singel stand, non reversing, 2 high rolling mill, having 135 mm diameter rolls, rotating at a fixed speed of 55 r.p.m. In case of Fe_3Al-Fe-Fe_3Al compacts, preheating was done at 1400 K for 10 min. in an inert atmosphere of either Ar or N_2, where as in case of Cu-Fe-Cu compacts preheating was done at 1273K for 5min. in dry H_2 atmosphere. The preheating furnace was interlinked with the rolling mill in such a manner that the strip remained in the protective atmosphere upto the roll nip. The set up for the hot rolling of hot pressed compacts under protective atmosphere is schematically shown in Fig.4.8. Thickness reduction was achieved by pulling the nichrome wire fastened to the compact and forcing it to pass through the rotating rolls set at a predetermined roll gap. Soon after rolling, the strips were cooled in a bed of fine graphite chips to prevent internal oxidation of the strip caused by the inter connected pores present in it. The strips behaved well during hot rolling and there was no significant edge cracking after rolling. However, after each rolling pass the cracked portion of the longitudinal edges of the strips were trimmed to avoid growth of these cracks in subsequent passes. The compacts were hot rolled to 20%, 40%, 60% and 80% thickness reduction.

4.5 Annealing of Hot Rolled Laminated Strip

During hot rolling the rolls were not preheated, therefore when hot strips came in contact with the cold rolls there was a chilling effect, in particular on the surface of the strip. This would bring down the temperature of the surface layer, leading to 'warm' working condition. Therefore, the densified strips after hotrolling were annealed. In case of Fe_3Al-Fe-Fe_3Al

strips annealing was done at 1400K for 45 min. in an inert atmosphere of Ar, where as in case of Cu-Fe-Cu strips annealing was done at 1273K for 45 min. in H_2 atmosphere. The strips were cooled in the cooling zone of the furnace under the protective atmosphere.

Fig.4.8: HOT ROLLING ARRANGEMENT

4.6 Characterization Methods

Mechanically alloyed Fe_3Al powder was subjected to X-ray diffraction studies and sieve analysis was carried out for all the metal powders. The hot pressed, hot rolled and annealed strips of Fe_3Al-Fe-Fe_3Al and Cu-Fe-Cu were tested for various mechanical and physical properties.

4.6.1 Sieve Analysis

Different metal powders used in the present study were characterized for particle size distribution by standard sieve analysis technique using the British Standard (B.S) sieves.

4.6.2 X-ray Diffraction Analysis

X-ray diffraction patterns for mechanically alloyed Iron aluminide powder was carried out on a X-ray diffractometer model RICH SIEFERT ISO DEBYEFLEX 2002, Germany. Cr-K_α radiation was used for the X-ray diffraction studies. The obtained diffraction patterns were compared with standard ASTM powder diffraction file data.

4.6.3 Scanning Electron Microscopy

Morphology of different metal powders were observed under JEOL JSM 840A, Scanning Electron Microscope(SEM). The fractured surface of the hot rolled and annealed strips were also studied with the help of SEM. The metal powder morphologies were observed by dispersing the powders with acetone on finely polished brass stubs prepared especially for this purpose. The fractured surfaces of the hot rolled and annealed strips were observed along the rolling direction.

4.6.4 Electron Micro Probe Analysis

Electron Micro Probe Analysis (EMPA) was conducted on a JEOL SUPERPROBE JXA 8600 MX, Electron micro probe analyzer. EMPA was done on the mechanically alloyed Fe_3Al powder to know the bulk composition of the powder.

4.6.5 Microhardness Testing

Microhardness of hotpressed compacts and hot rolled strips of Fe_3Al-Fe-Fe_3Al and Cu-Fe-Cu laminated strips was measured in a LEITZMINILOAD-2 micro hardness tester for hardness profiles. The micro hardness of hot pressed laminated compacts was measured on the cross-section. In case of hot rolled samples the micro hardness reading were taken on the transverse cross-section of the strip i.e. in the cross-section perpendicular to the rolling direction. 50 mN load was applied for the indentation purpose and the hardness was expressed in terms of HV scale of hardness.

4.6.6 Tension Testing

Ultimate tensile strength (UTS) and percentage of elongation were measured by uniaxial tension testing method on a INSTRON-1195 machine. The testing was done at room temperature and at a cross head speed of 0.5 mm/min for Cu-Fe-Cu laminated strips and at 0.2 mm/min for Fe_3Al-Fe-Fe_3Al laminated strips. The specimen used was not of standard specification as per BS18 specification [51]. However the geometry of the specimen as per above specification was maintained as shown in Fig.4.9.
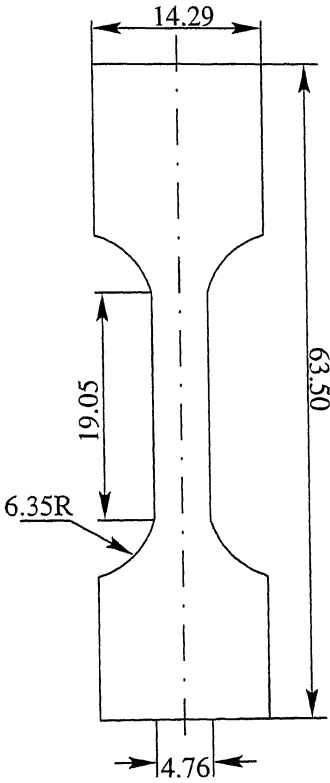
Fig.4.9 Tensile Test Specimen (units in mm) (Ref.51)

4.6.7 Density Measurements

Density of the hot rolled and annealed Fe_3Al-Fe-Fe_3Al and Cu-Fe-Cu laminated strips were measured by displacement method using the Archimedes principle.

Chapter 5

RESULTS AND DISCUSSION

5.1 Characterization of Mechanically Alloyed Iron Aluminide Powder

5.1.1 X-ray Diffraction

In Fe-Al binary system, up to 18at%, aluminum has good solid solubility in iron at room temperature. This fact made the room temperature mechanical alloying of Al with Fe less difficult. The X-ray diffraction pattern of Iron aluminide powder, mechanically alloyed for 24 hours, shows the peaks at 2θ values of 46,68,87 and 104, which is shown in Fig.5.1.

5.1.2 Size Distribution and Shape

The particle size distributaion of the iron aluminide powder was obtained from standard sieve analysis test . The particle size distribution is shown in Table-5.1 and in Fig.5.2. The shape of the Iron aluminide powder obtained in the present study is shown in the SEM photomicrograph in Fig.5.3.

5.1.3 Chemical Composition

The bulk chemical composition of the mechanically alloyed Iron aluminide powder was arrived at by conducting EMPA studies on a powder compact. The bulk chemical composition
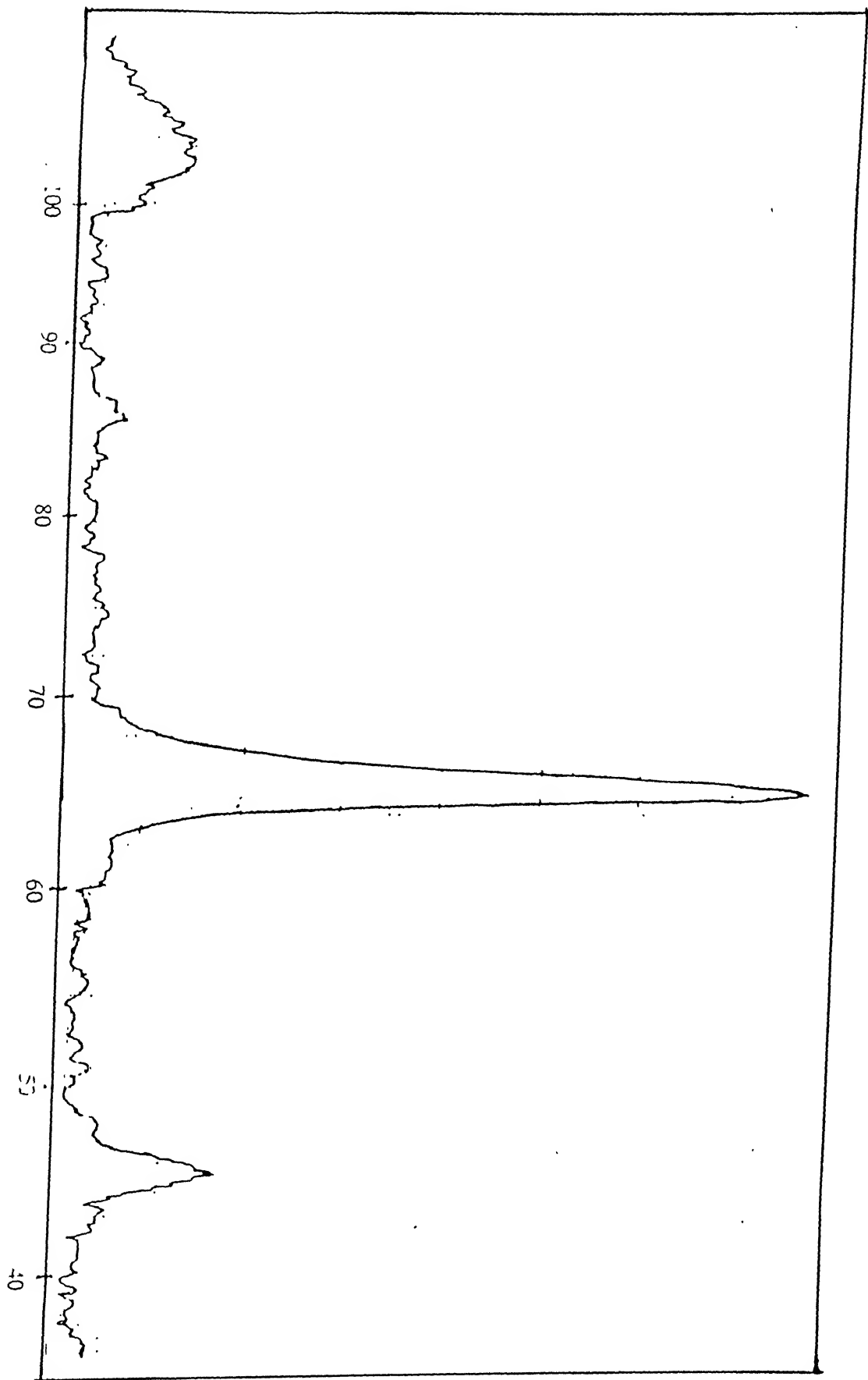
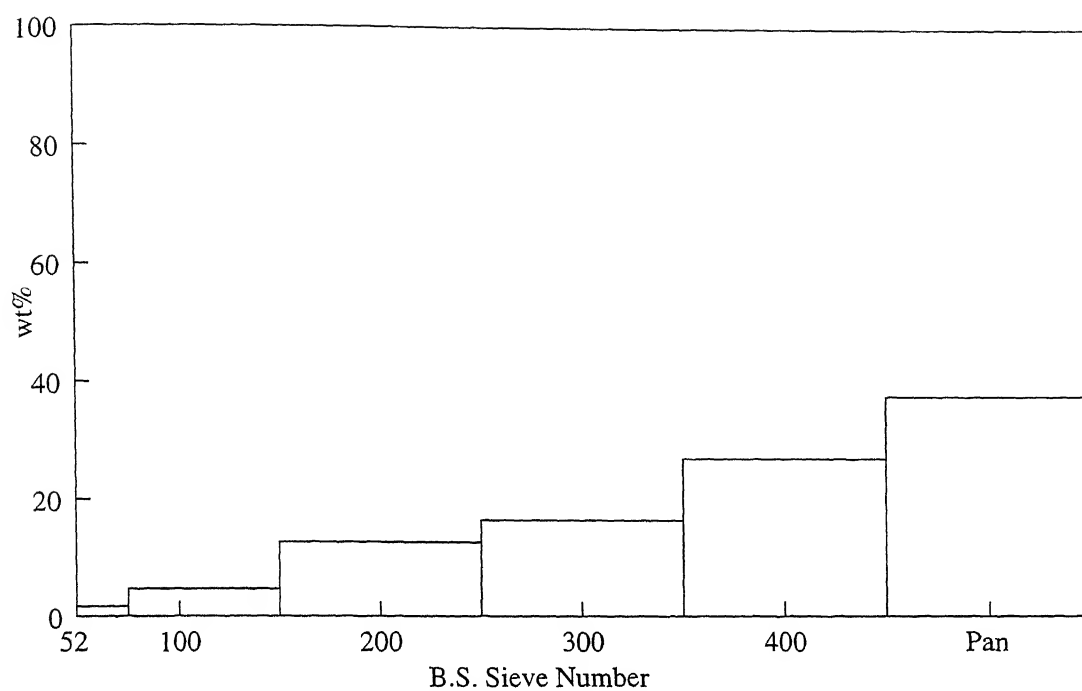Fig.5.1: X-ray diffraction pattern of mechanically alloyed Iron aluminide powder.

39

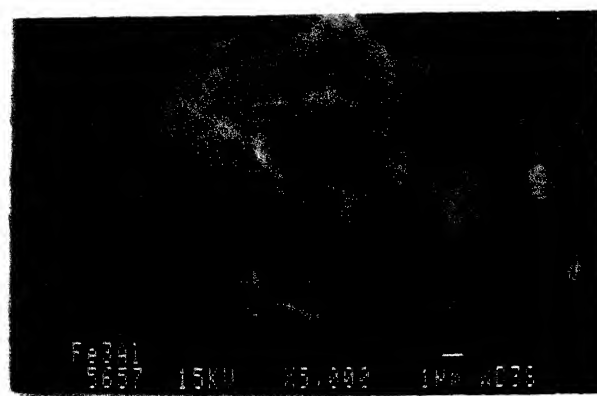Fig.5.2 : Partical size distribution of mechanically alloyed
Iron aluminide powder

Fig.5.3 : SEM Photomicrograph of mechanically alloyed iron aluminide powder

40

Table 5.1 : Particle Size Distribution of Mechanically Alloyed Fe$_3$Al Powder

B.S.Sieve Number	wt%
+52	1.69
+100	4.69
+200	12.67
+300	16.43
+400	26.99
+Pan	37.52

was calculated by taking the average of 10 test points is given in Table-5.2. The variation in the Iron content is from a minimum value of 81.96 wt% to a maximum value of 86.91 wt%, where as for aluminum it varies from a minimum value of 14.91 wt% to a maximum value of 17.30 wt%.

Table 5.2 : Chemical Composition of Mechanically Alloyed Fe$_3$Al

Constituent	Iron	Aluminum	Tungsten
wt%	84.49	15.41	0.10
at%	72.60	27.37	0.03

The staring material was Fe-13.95 wt% Al (i.e. Fe-25at%Al) powder aggregate but this composition could not be achieved in the final Iron aluminide powder because of relatively greater loss of Fe powder than Al powder through the shaft clearance in the planetry ball mill during milling operation. The reason for this differential loss could possibly be attributed to the finer particle size of the staring Fe powder, which had approximately 26 wt% of its powder mass below 300 mesh size, as compared to 19 wt% of Al powder below 300 mesh size (see section 4.1). A very little amount of tungsten is also appearing in the alloy. This may came from the worn out WC balls or WC container, used during mechanical alloying. The bulk carbon content could not be analyzed because of the technical limitation of the EMPA device.

5.1.4 Density

Theoretical density of Iron aluminide alloy of the composition obtained in the present study, is calculated by taking into consideration the individual contribution of the different constituents of the alloy powder (see Appendix-1).

5.2 Characterization of Fe₃Al-Fe-Fe₃Al Laminated Strip

5.2.1 Hot Pressing of Fe₃Al-Fe-Fe₃Al Compacts

The Fe₃Al-Fe-Fe₃Al laminated compacts used in the present study were hot pressed at a processing hold time of 30, 60, 120 min. while temperature and load were kept constant at 1223K and 1ton respectively.

5.2.1.1 Density of Hot Pressed Compacts

The variation in the density of Fe₃Al-Fe-Fe₃Al compacts with time is shown in Fig.5.4. Eventhough the density was increased with increase in the holding time, the maximum density obtained after 120 min was 5.67 g/cc, which is only 82.5% of the theoretical density. The theoretical density of the Fe₃Al-Fe-Fe₃Al is calculated by using the rule of mixtures (see Appendix-2). The reason for this low densification is attributed to the low values of temperature and pressure used during hot pressing. The temperature of hot pressing was less than $0.8T_m$ (Melting point) of Iron aluminide. Still higher densities may be achieved by increasing the temperature and pressure, during hot pressing.

5.2.1.2 Microhardness Profiles

The microhardness values measured across the Fe₃Al-Fe interface for 30, 60 and 120 min. hot pressed samples are plotted with distance to form the micro hardness line profiles which are shown in Fig.5.5 to 5.7. For each point an average of three readings on either side of the point were taken. Since the microhardness values are often associated with instrumental as
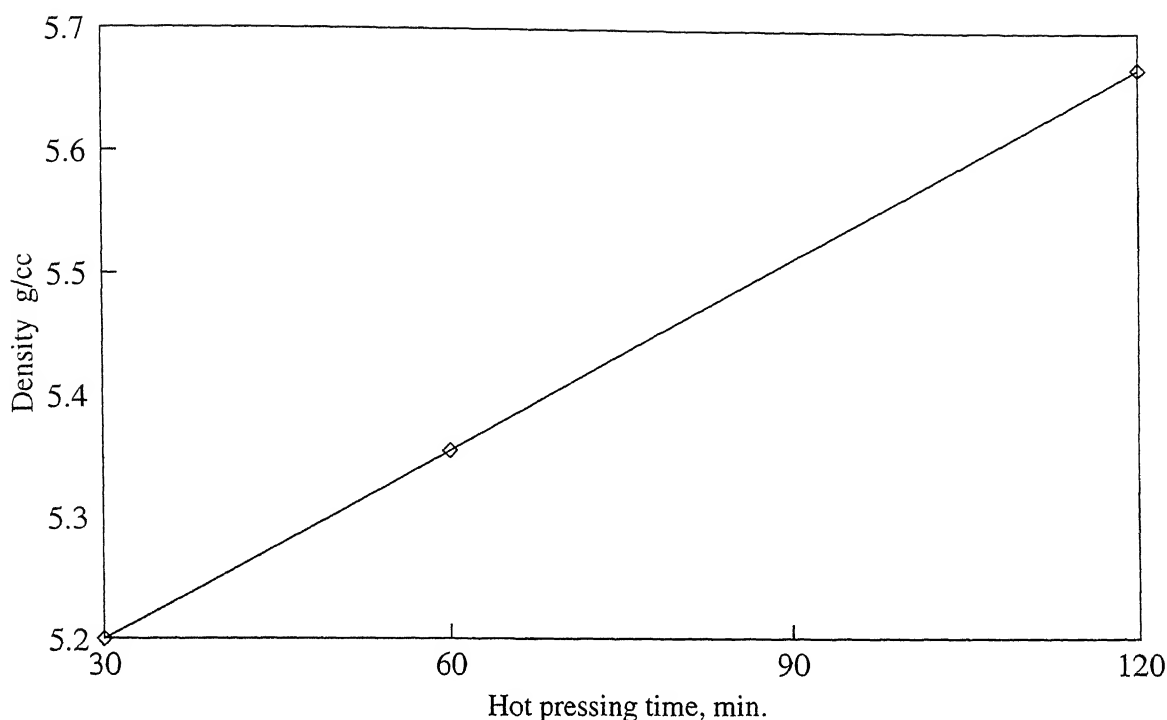
Fig.5.4 : Density variation with hot pressing time for
Iron aluminide-Iron-Iron aluminide compacts.

well as human error because of its very high sensitivity towards minimal fluctuation in the measuring conditions, these microhardness line profiles basically provide semi quantitative information. It was observed from these graphs that as the time of hot pressing increases the hardness values in the Fe_3Al area, Fe area and the interface area are increasing, which implies the densification of compacts. In the case of 30 min hot pressed sample the hardness values are so low, due to the presence of high porosity in the sample, which is over shadowing the hardness values of Fe_3Al and Fe.

5.2.2 Hot Rolling of Hot Pressed Fe_3Al-Fe-Fe_3Al Compacts

The compacts that were hot pressed for 120 min are selected for further densification and also to make the strips, by hot rolling. The compacts were hot rolled for 20%, 40%, 60% and 80% thickness reduction at 1423K, which are further studies for various physical and mechanical properties.
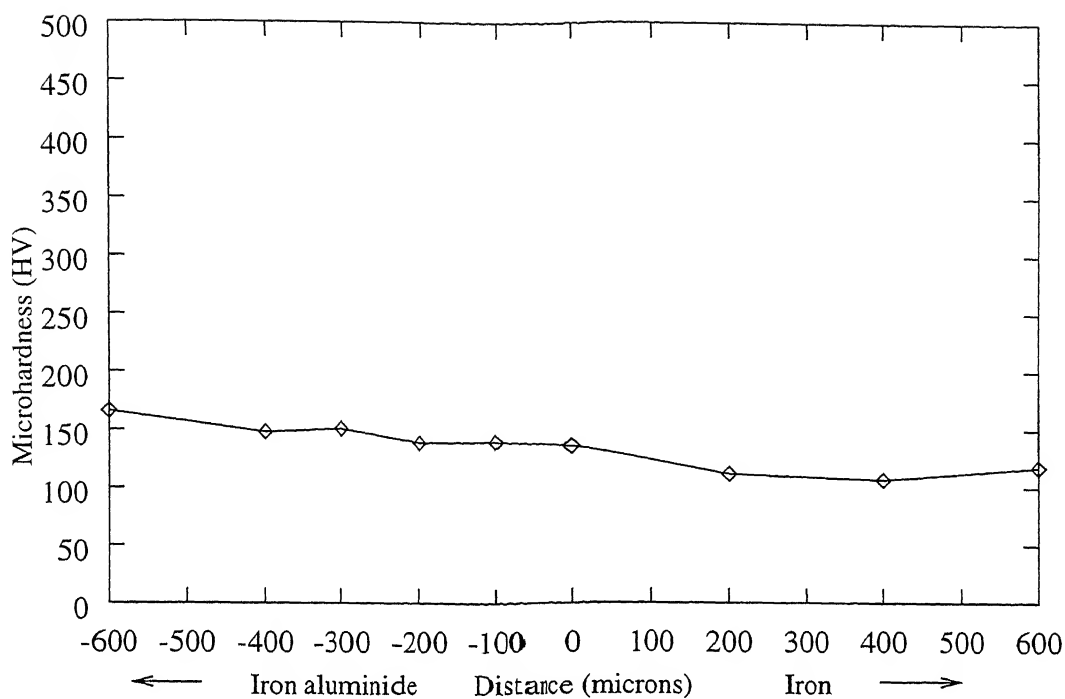
43

Fig.5.5 : Microhardness profile for 30 min. hot pressed
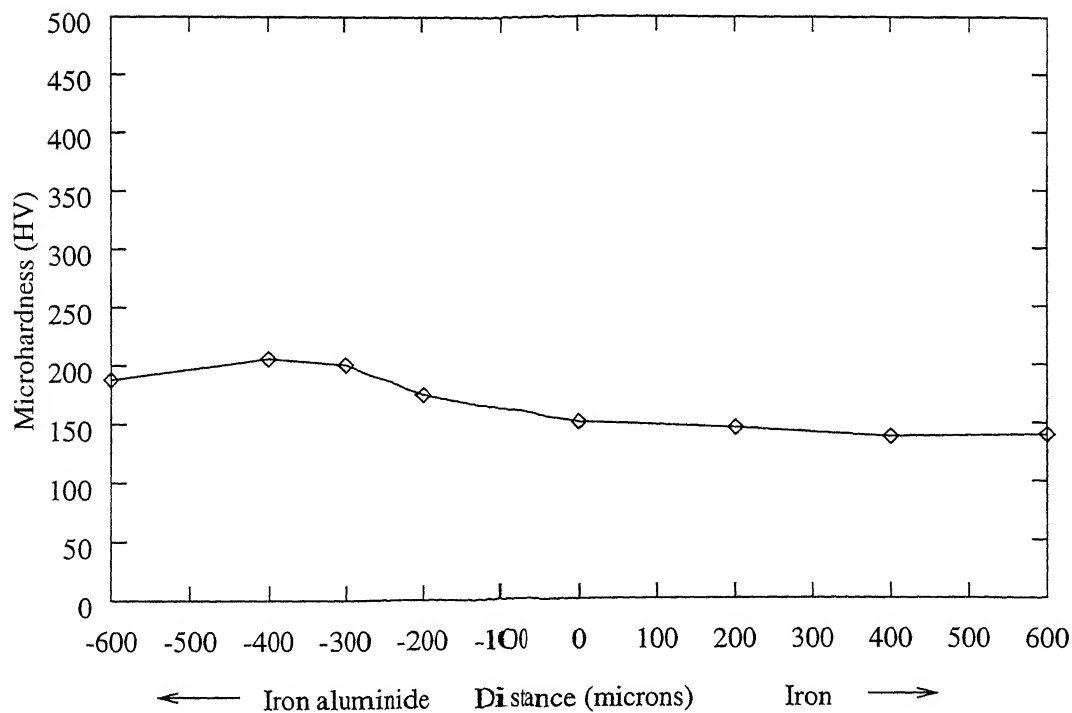Iron aluminide-Iron-Iron aluminide compact

Fig.5.6 : Microhardness profile for 60 min. hot pressed
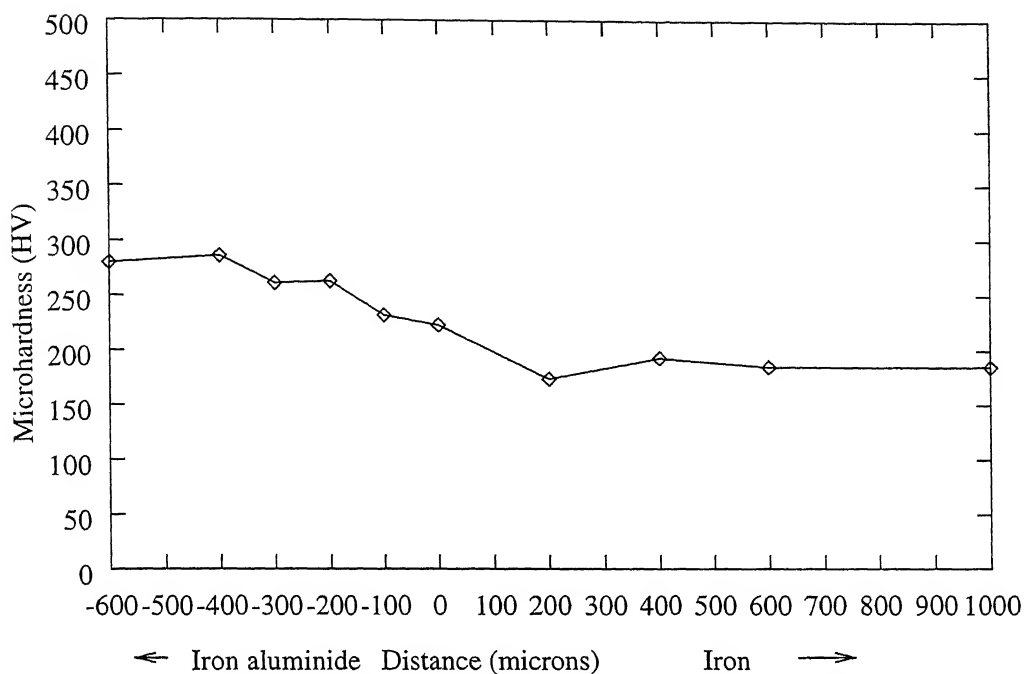Iron aluminide -Iron-Iron aluminide compact

44

Fig.5.7 : Microhardness profile for 120 min. hot pressed
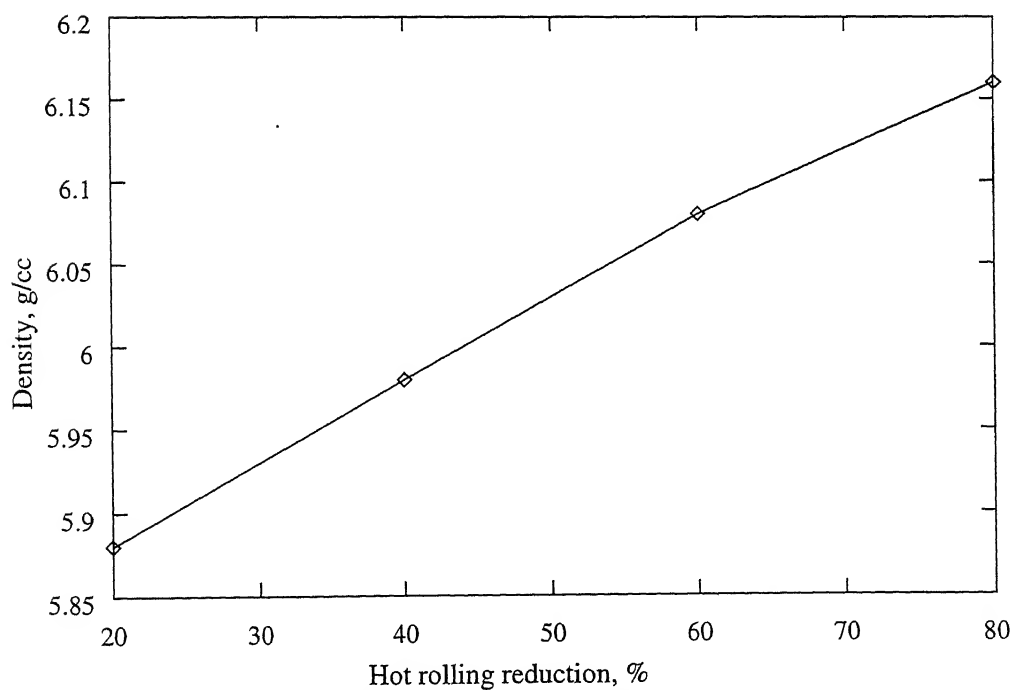Iron aluminide-Iron-Iron aluminide compact

Fig.5.8 : Density variation with hot rolling reduction for
Iron aluminide-Iron-Iron aluminide strips

45

5.2.2.1 Density

The change in density of strips with percentage of hot rolling is shown in Fig.5.8. The density of the strips was calculated by using immersion method. Even after 80% of thickness reduction the density obtained was only 90% of the theoretical. Further rolling may help in increasing the density, but it was not possible due to the development of cracks in the strip.

5.2.2.2 SEM of Fractured Laminated Fe_3Al-Fe-Fe_3Al Strips

The SEM photomicrographs of fractured Fe_3Al-Fe-Fe_3Al laminated strips are shown in Fig.5.9 to 5.11. Fig.5.9 (a), 5.10 (a) and 5.11 (a) shows the Fe_3Al surface of 40%, 60% and 80% hot rolled and fractured Fe_3Al-Fe-Fe_3Al laminated strip.The fractured surface of iron for 40%, 60% and 80% hotrolled specimen are shown in Fig.5.9 (b), 5.10 (b) and 5.11 (b).

It can be seen from SEM micrographs of the fractured surface of the 40% hotrolled Fe_3Al-Fe-Fe_3Al laminated composite strip (Fig.5.9 (a) and (b)) that the Fe_3Al powder particles have not elongated in the direction of rolling. Further, the iron layer shows ductile fractured surface, and very little porosity is present.

The SEM micrographs of the fractured surface of 60% hotrolled Fe_3Al-Fe-Fe_3Al laminated composite strip (Fig.5.10 (a) and (b)) shows that the Fe_3Al powder has been elongated in the direction of rolling, but still a large amount of porosity is present. The iron layer shows the typical ductile fracture.

The SEM micrographs of the fractured surface of 80% hotrolled Fe_3Al-Fe-Fe_3Al laminated composite strip (Fig.5.11 (a) and (b)) shows that the Fe_3Al powder has been further elongated in the direction of rolling, but complete densification has not taken place.

From the above observation, it is apparent that the Fe_3Al layer in the Fe_3Al-Fe-Fe_3Al laminated composite strip is not getting fully densified even after hot rolling to 80% thickness reduction, while Fe layer has become more or less fully densified.

The densification of porous metal strips by hot rolling occurs through the following mechanism.

1. Transitional restacking of particles.
2. Growth of contack area.
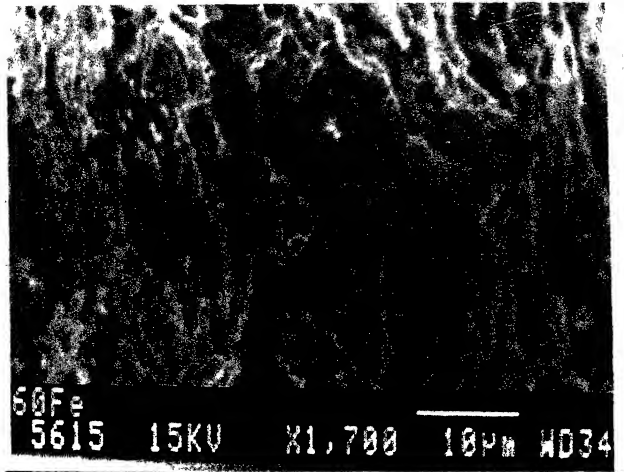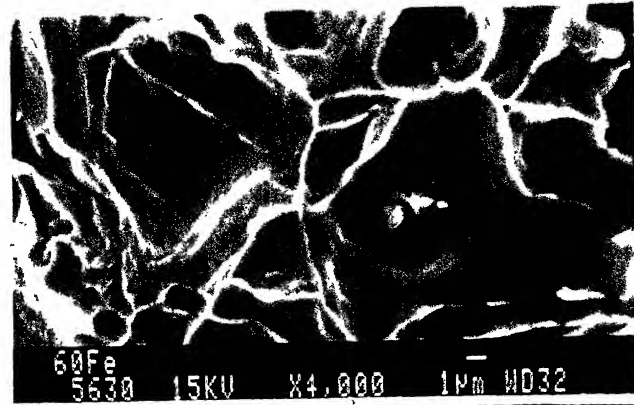3. longitudinal flow of particles in the rolling direction.
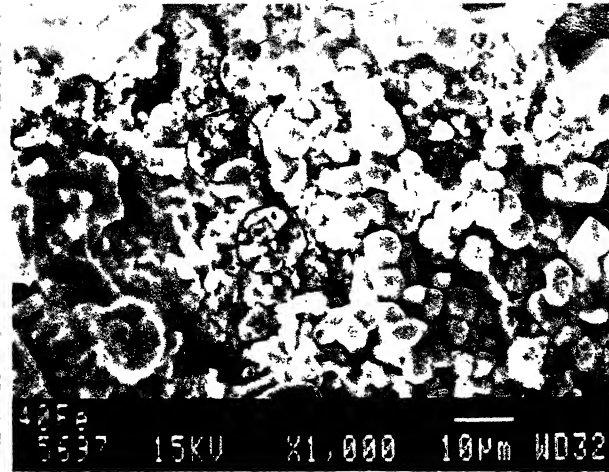
(a)
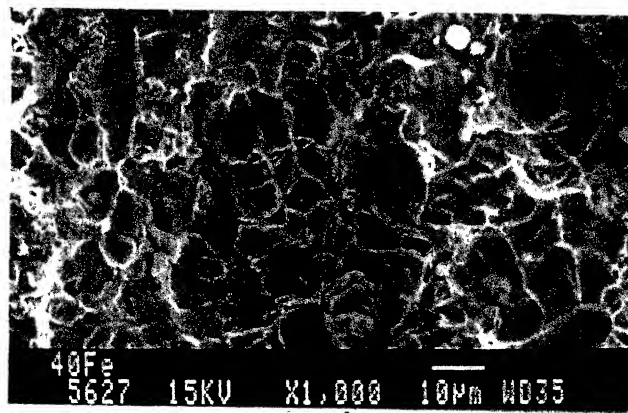
(b)

Fig.5.9 : SEM photomicrographs showing (a) Fe$_3$Al layer (b) Fe layer of 40% hotrolled and fractured Fe$_3$Al-Fe-Fe$_3$Al specimen.
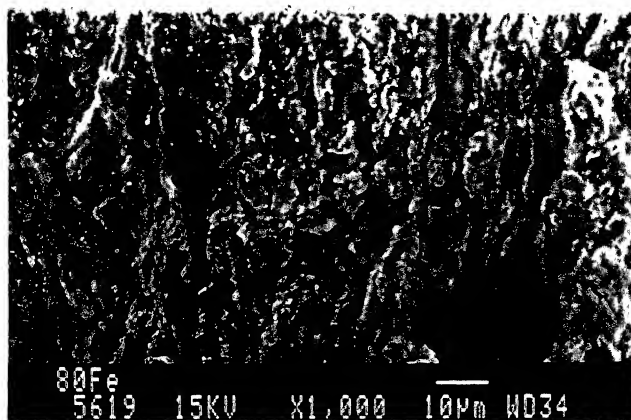
(a)
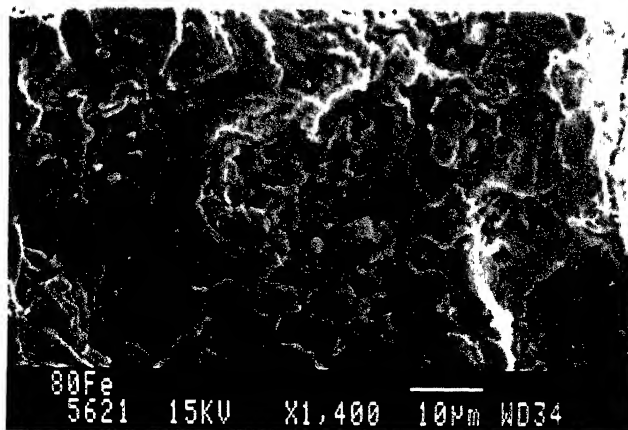

(b)

Fig.5.10 : SEM photomicrographs showing (a) Fe_3Al layer (b) Fe layer of 60% hotrolled and fractured Fe_3Al-Fe-Fe_3Al specimen.

48

(a)

(b)

Fig.5.11 : SEM photomicrographs showing (a) Fe_3Al layer (b) Fe layer of 80% hotrolled and fractured Fe_3Al-Fe-Fe_3Al specimen.

The overall stress acting on the strip during initial stages of deformation are, compressive in the thickness direction and tensile in the rolling direction. At the initial stages of deformation the powder particles rearrange and restack as the rolling progresses and the longitudinal elongation in this stage is negligibly small. The end of this stage is marked by a situation when no further densification with out longitudinal flow is possible by hot rolling. This situation corresponds to the closest packing among the powder particles and the relative density at which this occurs is a function of the initial size range of the metal powder. Some researches [51,52] have reported that this stage which is known as the stage-I of densification continues until a relative density of 0.70 has been achieved in the hot rolled strip for a particular size range powder. Densification from the relative density of 0.70 to 0.95 i.e. stage-II densification is associated with the continuous growth in the inter particle contact area and increase in longitudinal elongation as hot rolling progresses. In this stage, the inter connected porosity changes to the isolated one. Densification beyond the relative density of 0.95 i.e. stage-III densification takes place through pore fragmentation and collapsing of the opposite pore surfaces until complete annihilation of porosity.

In case of Fe_3Al powder the stage-II densification lies somewhere between 40% and 60% thickness reduction (from Fig.5.9 (a) and 5.10 (a)), where as in case of Fe stage-II densification achieved before 40% thickness reduction.

5.2.2.3 Microhardness Profiles

The microhardness values measured across the Fe_3Al-Fe interface at different degrees of hot rolling reduction are plotted with distance to form microhardness line profiles which are in Fig.5.12 to 5.15.From these profiles we can observe that the hardness values of iron are reached to a constant level, at 40% of thickness reduction where as the hardness values of iron aluminide are increasing from 40% to 80% thickness reduction.

5.2.2.4 Mechanical Properties

The room temperature mechanical properties of 80% hot rolled and annealed Fe_3Al-Fe-Fe_3Al laminated strip found out by the tension test are shown in Table-5.3.
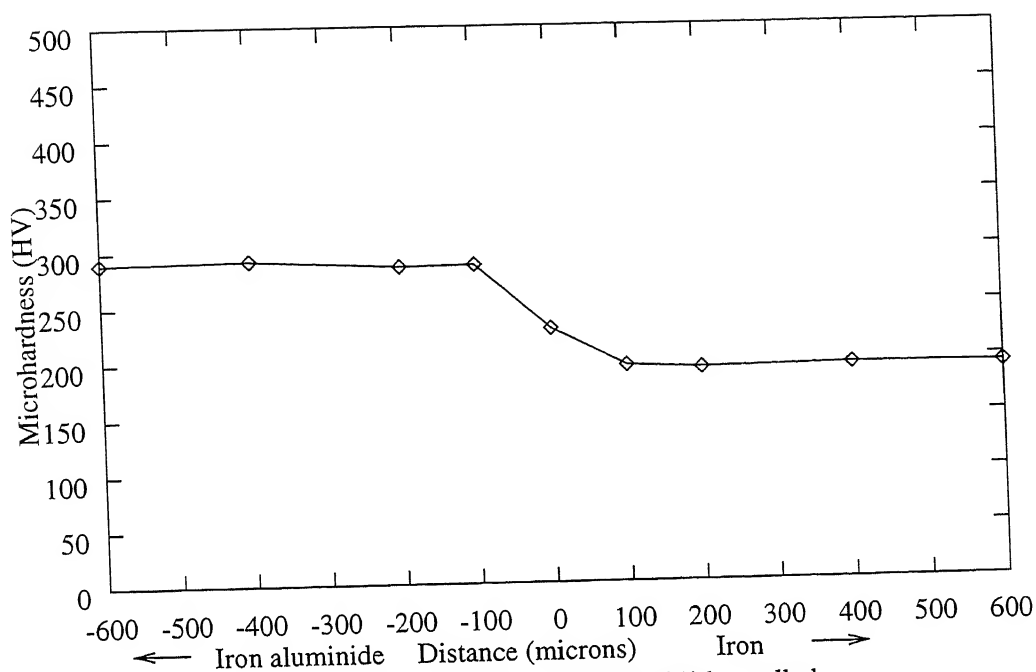
Fig.5.12 : Microhardness profile for 20% hot rolled
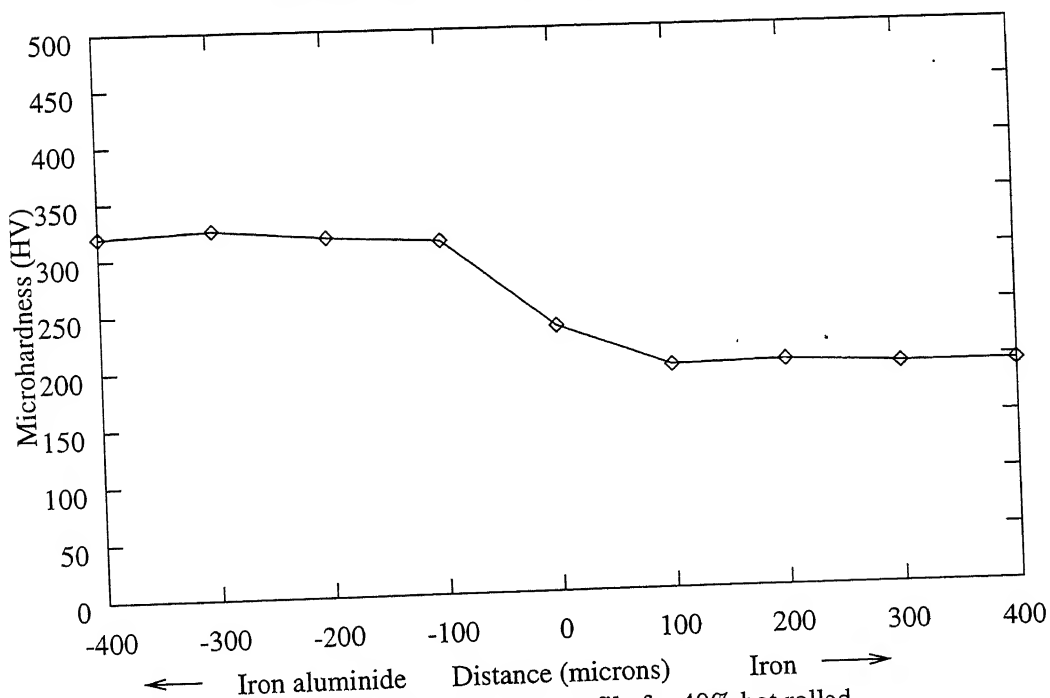Iron aluminide-Iron-Iron aluminide strip

Fig.5.13 : Microhardness profile for 40% hot rolled
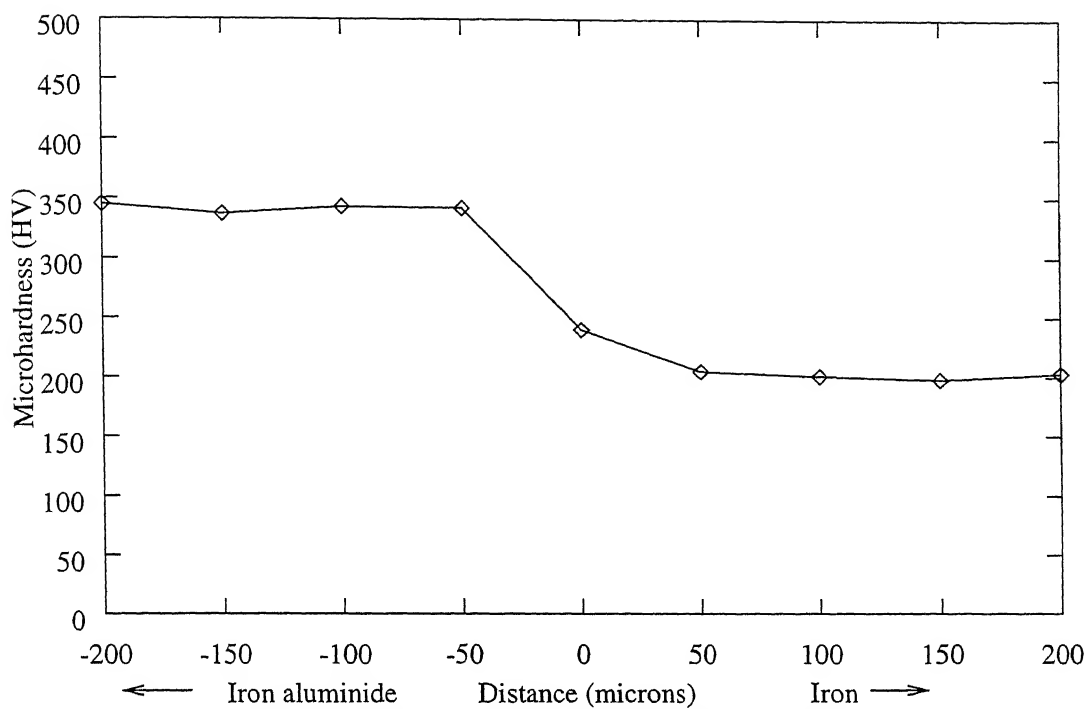Iron aluminide-Iron-Iron aluminide strip

51

Fig.5.14 : Microhardness profile for 60% hot rolled
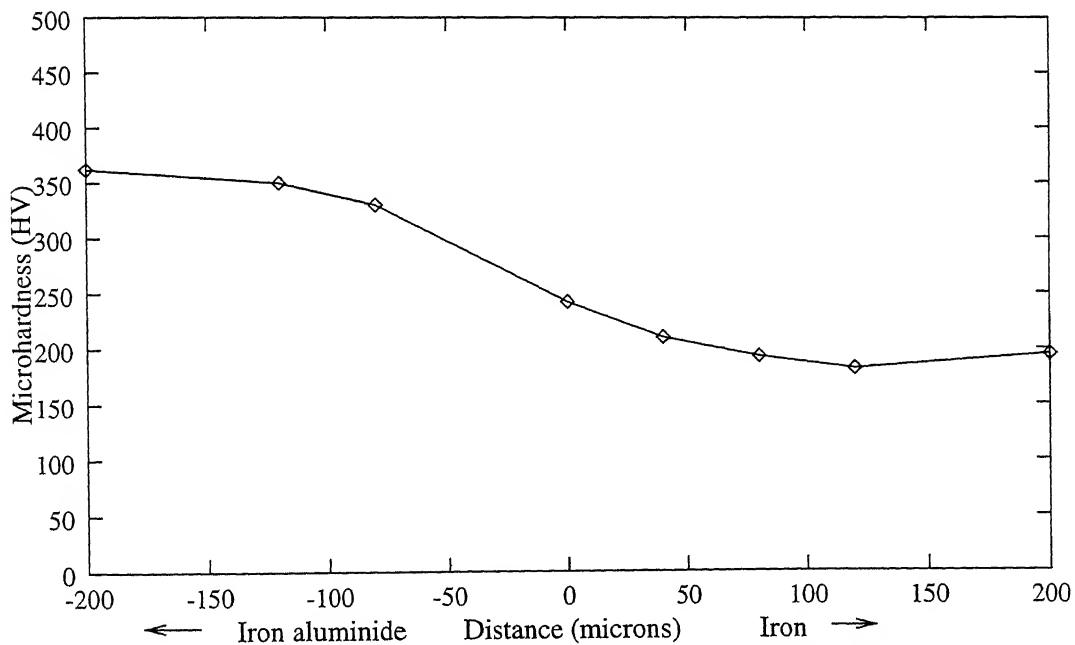Iron aluminide-Iron-Iron aluminide strip

Fig.5.15 : Microhardness profile for 80% hot rolled
Iron aluminide-Iron-Iron aluminide strip

The mechanical properties of cast, hotrolled and annealed monolithic Fe_3Al of composition corresponds to Fe-28 at%Al are given in Table-5.4. The ultimate tensile strength (U.T.S) and ductility of the Fe_3Al-Fe-Fe_3Al laminated strip are poor as compared to the monolithic Fe_3Al. This may be due to the low densification level observed in the iron aluminide layer and also due to the weak interfacial bonding between the iron and iron aluminide layers which leads to delamination. This is apparent from Fig.5.16 (a) which shows crack at the interface of Fe_3Al and Fe in fractured 80% hot rolled sample.The evidence of delamination during mechanical testing is shown in Fig.5.16 (b).

Table 5.3 : Mechanical Properties of Fe_3al-Fe-Fe_3Al Laminated Strip

Property	Values
U.T.S (MPa)	197
%Elongation	2

Table 5.4 : Mechanical Properties of Hot rolled and Annealed Fe-28 at% Al

| Property	Value	Ref.
U.T.S (MPa)	514	44
%Elongation	3.7	44

5.3 Characterization of Cu-Fe-Cu Laminated Strip

5.3.1 Hot Pressing of Cu-Fe-Cu Compats

The Cu-Fe-Cu laminated compacts used in the present study were hotpressed at a processing hold time of 30, 60, 120 min.,while temperature and load were kept constant at 1173K and 1ton respectively
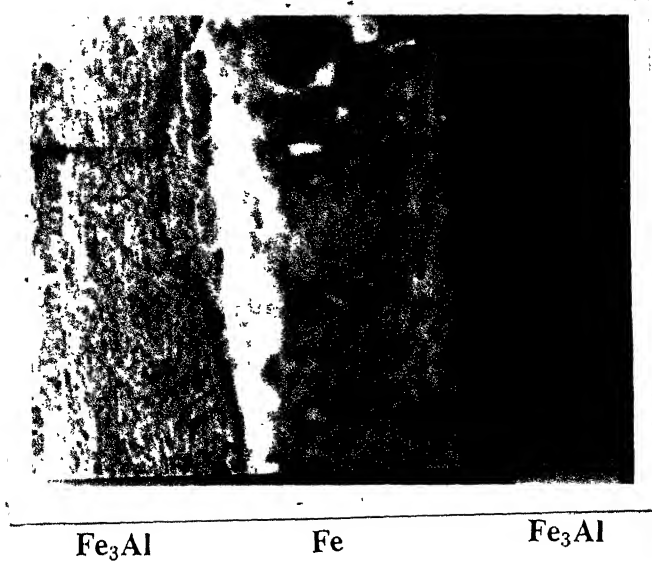
5.3.1.1 Density of Hot Pressed Compacts

The variation in density of Cu-Fe-Cu compacts with time is shown in Fig.5.17. The density of the compact after 120 min. of hot pressing was 7.9 g/cc which is ~ 94% of the theoretical density of the Cu-Fe-Cu compact of the composition chosen for the present study.

53

Fe

Fe$_3$Al

(a)

Fe$_3$Al   Fe   Fe$_3$Al
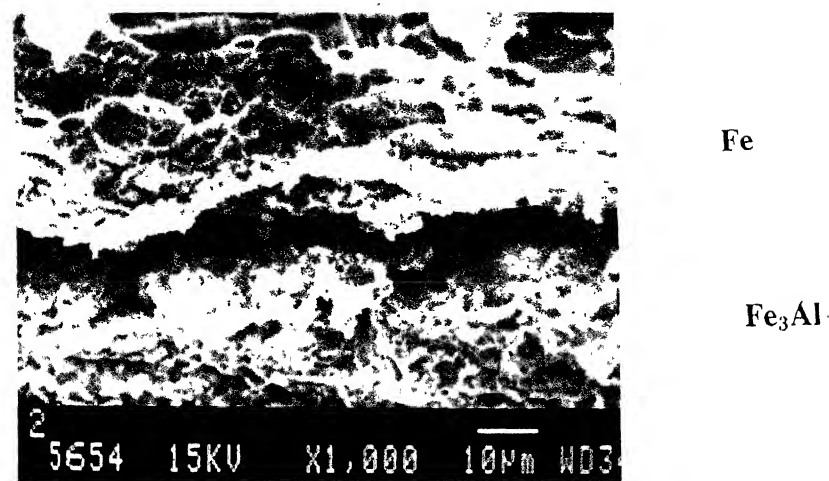
(b)

Fig.5.16 : SEM photomicrographs of (a) 80% hot rolled and fractured (b) tensile speci-
men at the interface.

54

The theoretical density of the compact was calculated by using the rule of mixtures(See Appendix-2).

5.3.1.2 Microhardness Profiles

The microhardness values measured across the Cu-Fe interface for 30, 60, 120 min. hot pressed samples are plotted against distance to form the microhardness line profiles, which are shown in Fig.5.18 to 5.20. It was observed from these profiles that as the time of hot pressing increases, the hardness values in the Cu area, Fe area and the interface area are increasing. This is obviously due to greater densification as the hot pressing time increases.

5.3.2 Hot Rolling of Hot Pressed Cu-Fe-Cu Compacts

Further hot densification rolling was carried out on Cu-Fe-Cu compacts hot pressed at 1173K for 120 min. The compacts were hot rolled for 20%, 40%, 60% and 80% thickness reduction at 1273K, which are further studied for various physical and mechanical properties.

5.3.2.1 Density of Hot Rolled Strips

The density of the hot rolled Cu-Fe-Cu strips against the percentage of hot rolling reduction is shown in Fig.5.21. The density of strips was calculated by using immersion method. Maximum density was obtained in case of 80% hot rolled Cu-Fe-Cu strips, which is about 98% of theoretical density.

5.3.2.2 SEM of Fractured Laminated Cu-Fe-Cu Strip

The SEM photomicrographs of fractured Cu-Fe-Cu laminated strips are shown in Fig.5.22 to 5.24. Fig.5.22 (a), (b) and (c) shows the Cu surface of 20%, 40% and 80% hot rolled and fractured Cu-Fe-Cu laminated strips respectively. The fractured surface of iron for 20%, 40% and 80% hotrolled specimen are shown in Fig.5.23 (a), (b) and (c) respectively. Fig.5.24 shows the Fe-Cu interface of the 80% hot rolled and fractured sample.
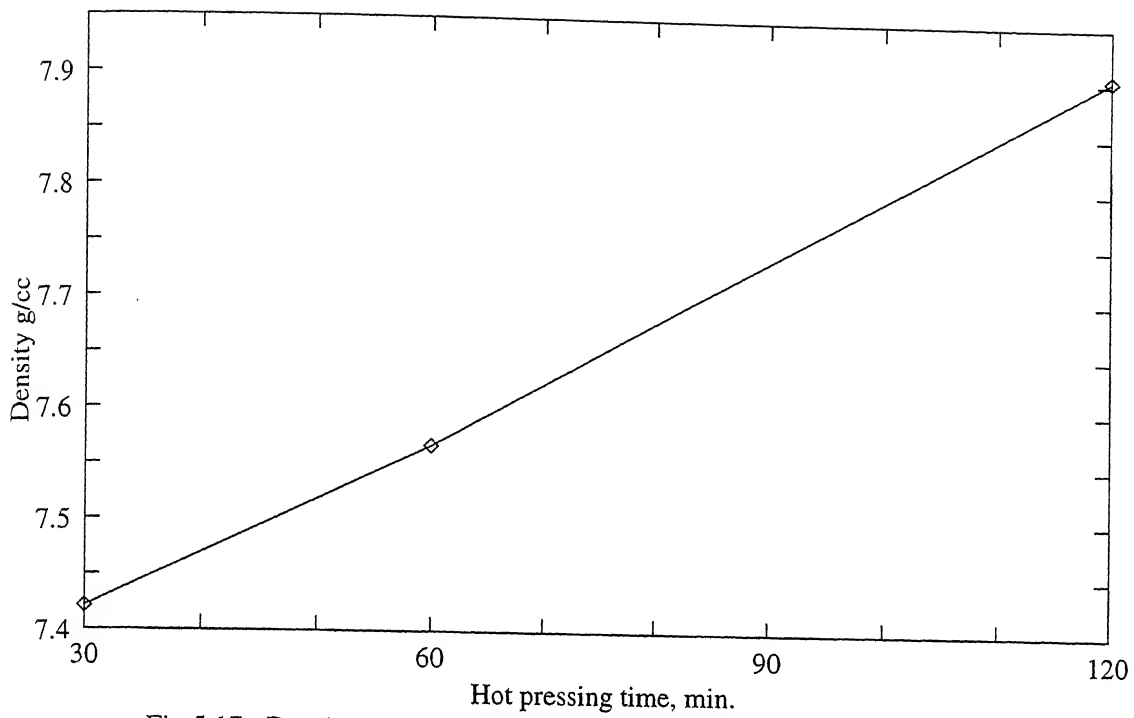
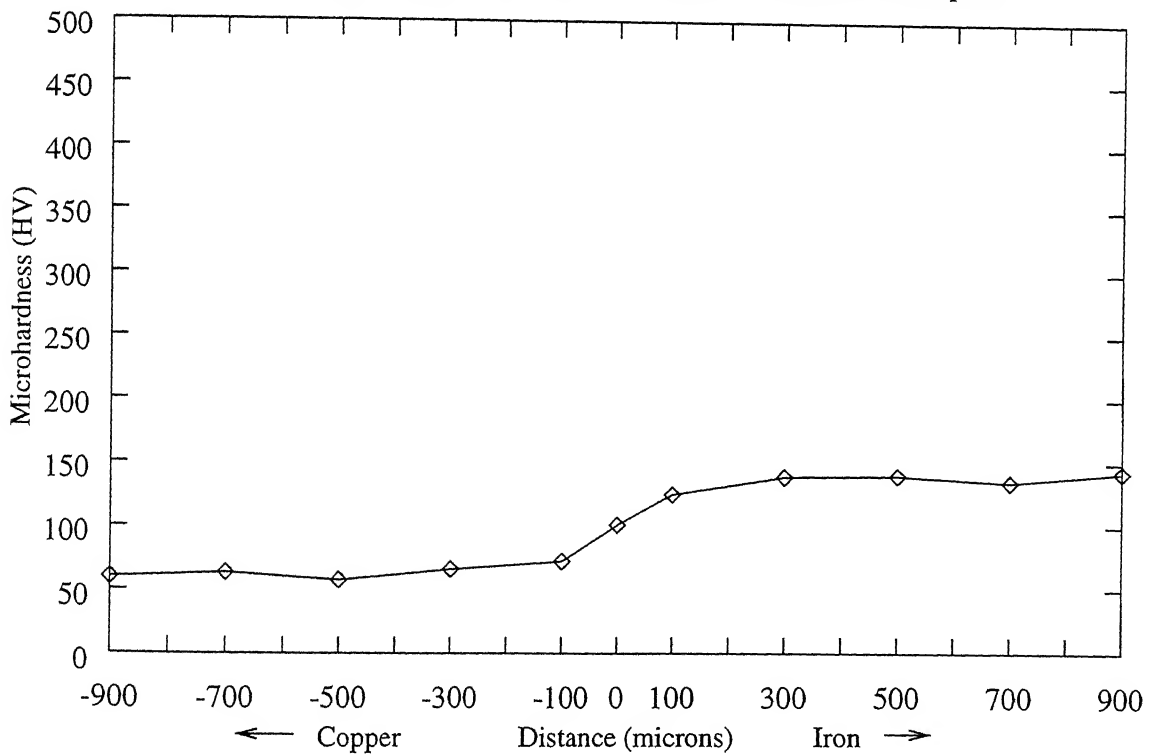Fig.5.17 : Density variation with hot pressing time for Cu-Fe-Cu compacts

Fig.5.18 : Microhardness profile for 30 min. hot pressed Cu-Fe-Cu compact
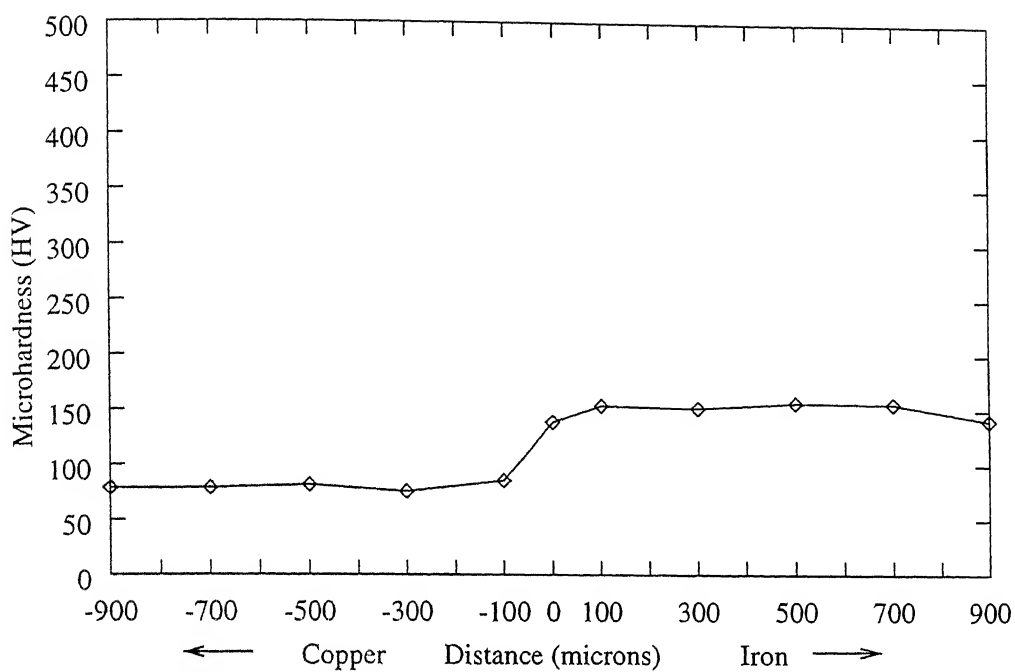
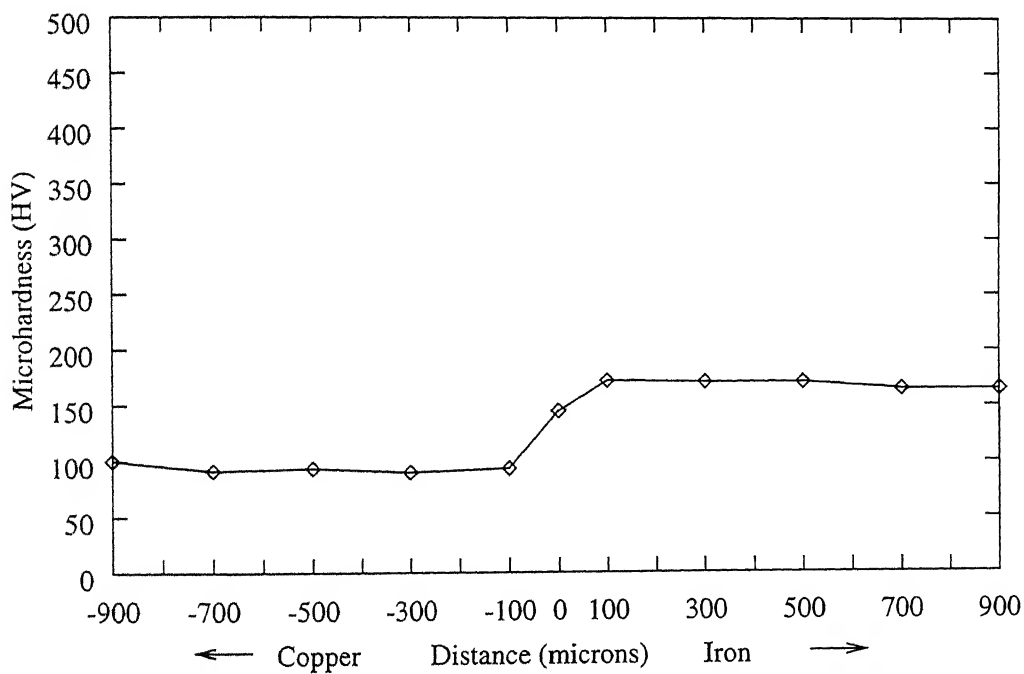Fig.5.19 : Microhardness profile for 60 min. hot pressed Cu-Fe-Cu compact

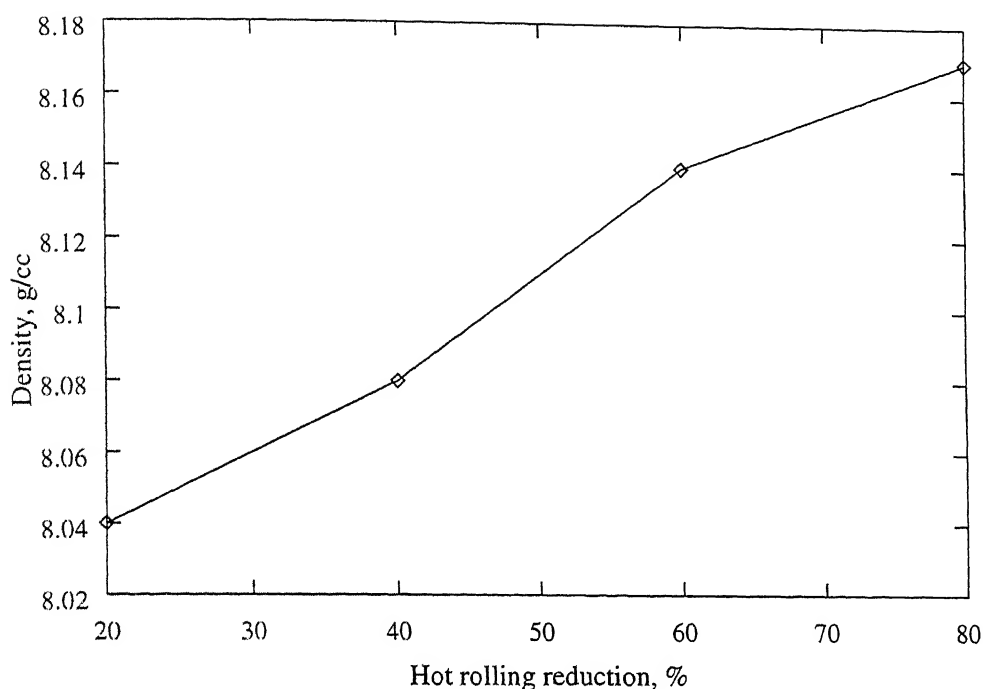Fig.5.20 : Microhardness profile for 120 min. hot pressed Cu-Fe-Cu compact

Fig.5.21 : Density variation with percentage of hot rolling
reduction for Cu-Fe-Cu strips

It can be seen from the SEM micrographs of the fractured copper surface of the Cu-Fe-Cu laminated composite that 20% of hot rolling (Fig.5.22 (a)) Cu layer shows ductile fractured surface. Similar behavior can be observed for the specimens hot rolled to 40% and 80% thickness deformation.

The SEM micrographs of the fractured Fe surface of Cu-Fe-Cu laminated composite (Fig.5.23) also shows the typical ductile fracture. After 120 min. of hot pressing the laminate attains 94% of it's theoretical density, which implies the isolation of interconnected porosity. This closed porosity would be removed by pore fragmentation and collapsing of opposite pore surfaces, which is Stage-III of densification, during hotrolling. The densification behavior in Cu and Fe layer are more or less similar, as evident from Fig.5.22 and 5.23.

5.3.2.3 Microhardness Profiles

The microhardness profiles along the Cu-Fe interface for 20%, 40%, 60% and 80% thickness reduction are shown in Fig.5.25 to 5.28.

58
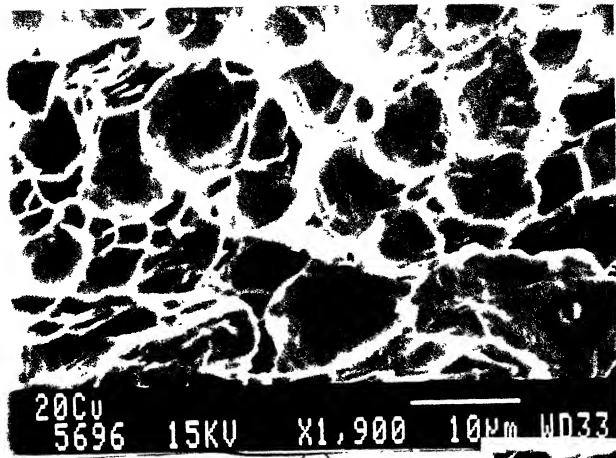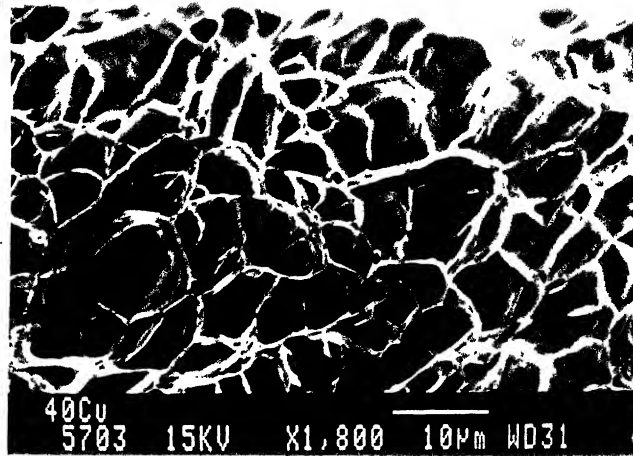
Fig 5.22 : SEM photomicrographs showing Cu layer of (a) 20% (b) 40% and (c) 80% hot rolled and fractured samples.

59

(a)

(b)
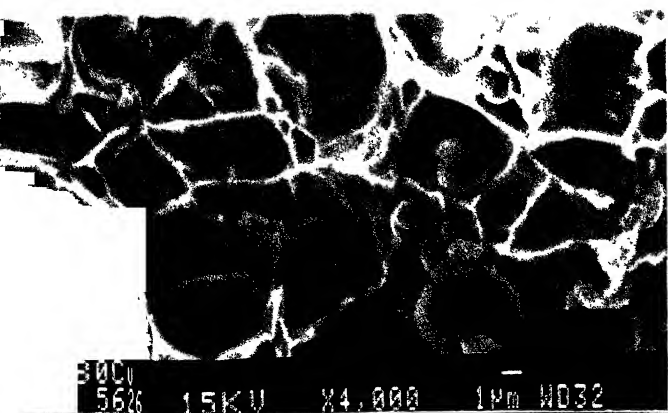
(c)

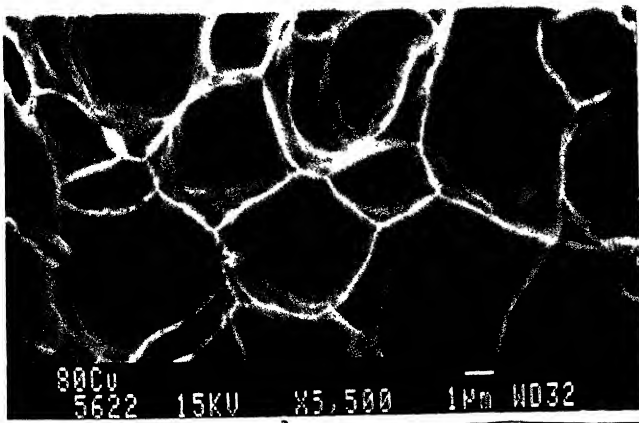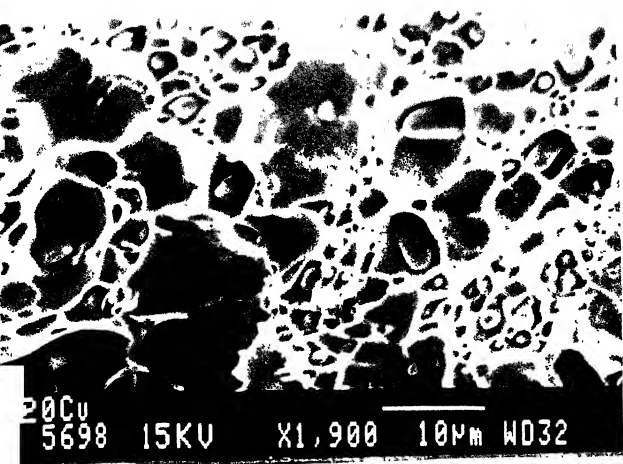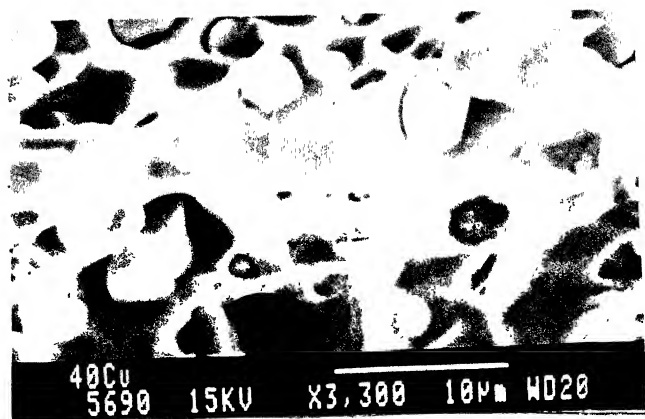Fig 5.23 : SEM photomicrographs showing Fe layer of (a) 20% (b) 40% and (c) 80% hot rolled and fractured samples.

<div align="center">Fe   Cu</div>
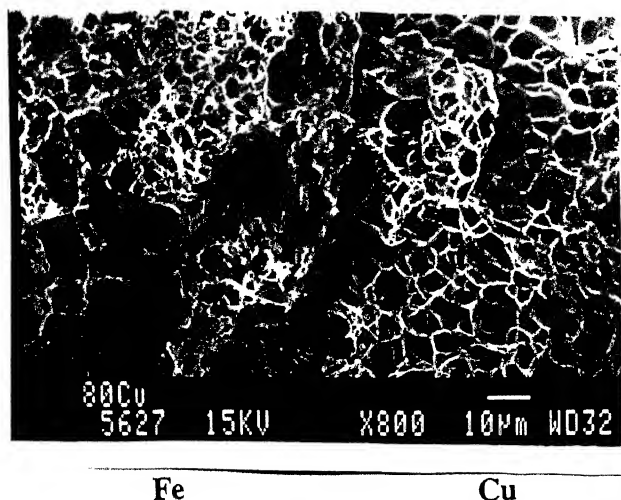
Fig 5.24 : SEM photomicrograph showing Cu-Fe interface of 80% hot rolled and fractured sample.

From these profiles it can be observed that the microhardness values in the copper area remains more or less constant and does not change with percentage thickness reduction by hot rolling. On the other hand, the microhardness values in the iron area increases with hot rolling reduction up to 40% thickness reduction, and then remains constant.

5.3.2.4 Mechanical Properties

The room temperature mechanical properties of 80% hot rolled and annealed Cu-Fe-Cu laminated strip found out by tension testing are shown in Table-5.5. The theoretical values of Ultimate tensile strength and percentage of elongation for Cu and Fe are shown in Table-5.6 [53].

<div align="center">

Table 5.5 : Mechanical Properties of Cu-Fe-Cu Laminated Strip

Property	Value
U.T.S (MPa)	275
%Elongation	9

</div>

Fig.5.27 : Microhardness profile for 60% hot rolled Cu-Fe-Cu strip
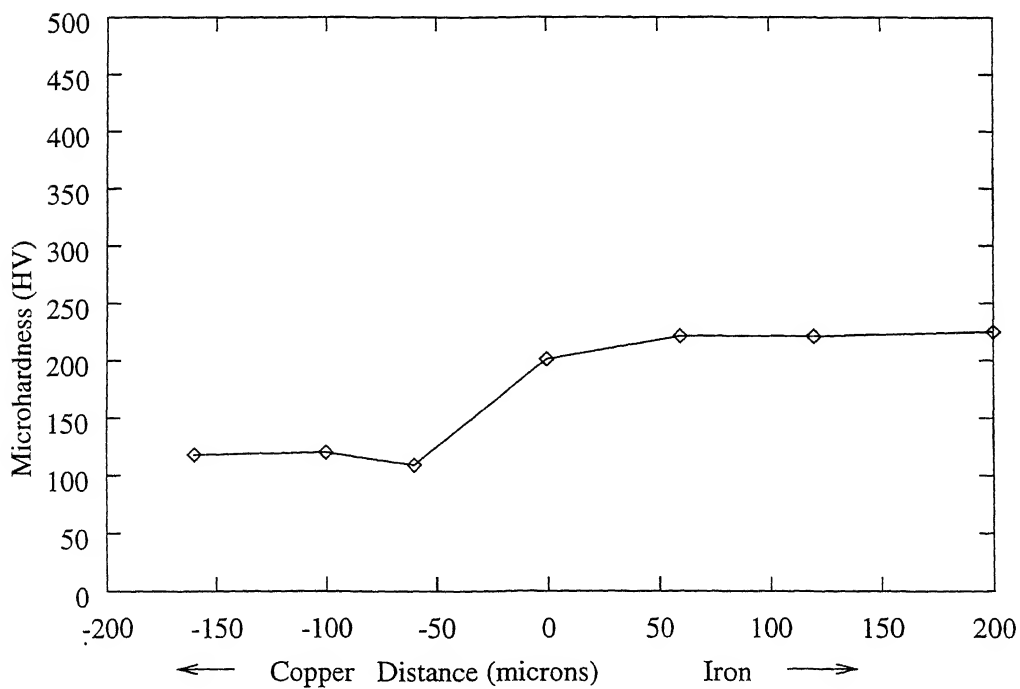
Fig.5.28 : Microhardness profile for 80% hot rolled Cu-Fe-Cu strip

Table 5.6 : Theoretical Mechanical Properties of Cu & Fe

Material	U.T.S (MPa)	% Elongation	Ref.
Cu (BS 2870)	200	35	53
Fe (BS 858)	340	21	53

The experimentally obtained strength value of the laminate is exactly matching with the theoretical strength value of Cu-Fe-Cu l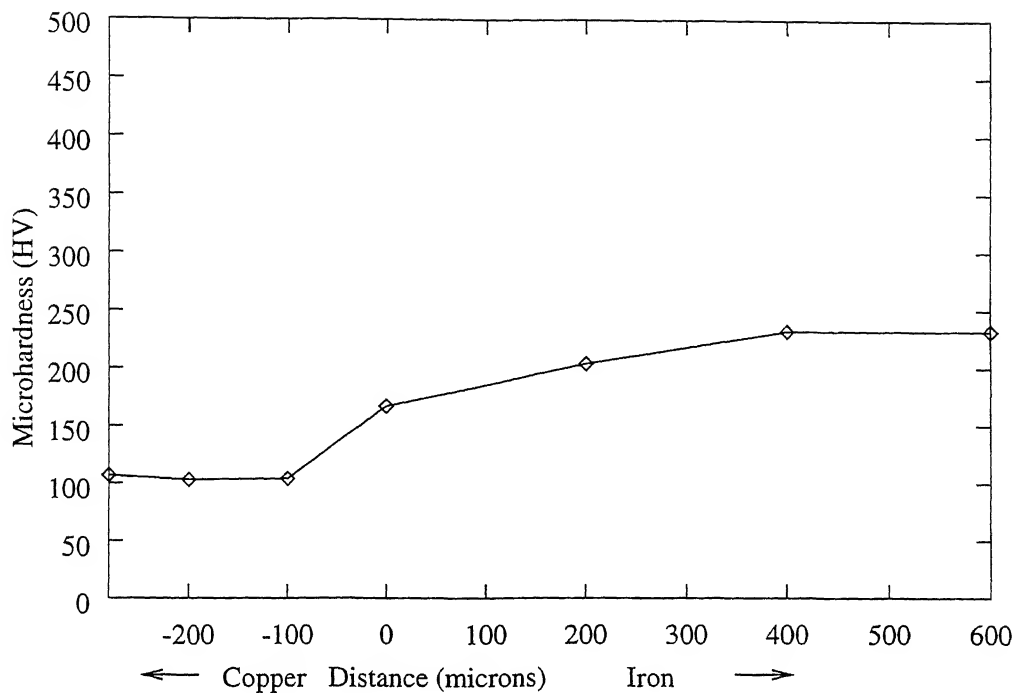aminate. The theoretical U.T.S. value of the laminate was found out by using rule of mixtures (See Appendix-3), which is about 273 MPa. The ductility of the Cu-Fe-Cu laminate is very less as compared to either Cu or Fe. This low ductility of the laminated strip is possibly attributed to the presence of some brittle phase at the interface leading to the problem of delamination as shown in Fig.5.24.

5.4 Cu-Ni-Fe-Ni-Cu Laminated Strip

In order to improve the ductility of the Cu-Fe-Cu laminated strip Ni was introduced between Cu and Fe on both sides. Introduction of Ni between Cu and Fe enhances the interfacial bonding. The mechanical properties of 85% hot rolled and annealed Cu-Ni-Fe-Ni-Cu laminated strip are shown in Table-5.7.

Table 5.7 : Mechanical Properties of Cu-Ni-Fe-Ni-Cu Laminated Strip

Property	Value
U.T.S (MPa)	293
% Elongation	19

64

Chapter 6

CONCLUSIONS

1) Fe$_3$Al-Fe-Fe$_3$Al and Cu-Fe-Cu laminated composite compacts have successfully been formed by hot pressing.In case of Fe$_3$Al-Fe-Fe$_3$Al the density achieved was 83% of the theoretical density when hot pressing was done at 1223K for 120 min. In case of Cu-Fe-Cu laminated composite compacts the density achieved was 94% of it's theoretical density when hot pressing was done at 1173K for 120 min. Still higher densities can be achieved in both cases by increasing temperature and pressure during hot pressing.

2) Fe$_3$Al-Fe-Fe$_3$Al laminated composite compacts can successfully be hot rolled at 1423K, up to 80% thickness reduction with out any significant edge cracking. There was no visible surface cracks on the Fe$_3$Al layer after hot rolling.

3) Fe$_3$Al-Fe-Fe$_3$Al laminated composite strips having thickness 28 %Fe$_3$Al on both sides of Fe layer obtained by hot rolling Fe$_3$Al-Fe-Fe$_3$Al composite compacts at 1423K to 80% thickness reduction followed by annealing at 1423K for 45 min. in Ar atmosphere, have tensile strength of 197 MPa coupled with an elongation of 2%

4) Cu-Fe-Cu laminated composite compacts can be successfully be hot rolled at 1273K even beyond 80% thickness reduction with out any significant edge cracking.

5) Cu-Fe-Cu laminated composite strip having 24 thickness % Cu on both sides of Fe layer obtained by hot rolling Cu-Fe-Cu composite compacts at 1273K to 80% thickness reduction followed by annealing at 1273K for 45 min. in H2 atmosphere, have a tensile strength of 275 MPa coupled with an elongation of 9%. Even though, the strength value of Cu-Fe-

65

Cu laminated strip is exactly matching with the theoretical strength value, obtained by rule of mixtures,the ductility is very poor perhaps due to some brittle phase formation at the interface.

6) In order to improve the ductility of Cu-Fe-Cu laminated strip a Ni layer can be added between Cu and Fe on both sides, which enhances the interfacial bonding. The Cu-Ni-Fe-Ni-Cu laminated strip has a tensile strength value of 293 MPa and a tensile elongation to failure of 19%

Chapter 7

SUGGESTIONS FOR FUTURE WORK

1) Work is needed for improving the interfacial bonding between Iron aluminide and Iron. This could be accomplished by increasing the temperature and percentage hot rolling thickness reduction.

2) Further investigations can be done on the corrosion resistance of Fe_3Al-Fe-Fe_3Al laminated composite strips in various atmospheres and at various temperatures.

APPENDIX

1. Calculation of Theoretical Density of Iron aluminide

The theoretical density of the mechanically alloyed Iron aluminide is calculated using the following formula

$$\rho_{Fe_3Al} = \frac{W_{Fe}+W_{Al}+W_W}{\frac{W_{Fe}}{\rho_{Fe}}+\frac{W_{Al}}{\rho_{Al}}+\frac{W_W}{\rho_W}} = \frac{\sum W_i}{\sum \frac{W_i}{\rho_i}}$$

Where,

ρ_{Fe_3Al} =Theoretical density of Iron Aluminide,

W_i = Weight fraction of 'i' element,

ρ_i = Theoretical density of 'i' element.

In the present calculation ρ_{Fe}, ρ_{Al} and ρ_W are taken to be 7.89, 2.70 and 19.3 g/cc respectively which yielded a theoretical density value of 6.09 g/cc. The respective W_i are calculated from the final composition of mechanically alloyed Iron aluminide powder (see Table-5.2).

2. Calculation of Theoretical Density of Laminated Strips

The theoretical density of Fe_3Al-Fe-Fe_3Al and Cu-Fe-Cu laminated strips is calculated using the following formula.

$$\rho_L = \frac{m_x+m_y}{\frac{m_x}{\rho_x}+\frac{m_y}{\rho_y}}$$

Where,

ρ_L = Theoretical density of the laminated strip,

m_x and m_y = Mass of the constituent elements 'x' and 'y' respectively,

ρ_x and ρ_y = Density of 'x' and 'y' respectively.

3. calculation of the Composite Mechanical Properties of Cu-Fe-Cu Laminated Strip

The composite mechanical properties of Cu-Fe-Cu laminated strip is calculated by using the rule of mixtures. The formula used is,

$$P_M = t_{Cu}P_{Cu} + t_{Fe}P_{Fe} = \sum t_i P_i$$

Where,

P_M = A particular mechanical property of the laminated strip,

t_i = Total thickness fraction of the 'i' constituent,

Now, taking avarage thickness ratio of Cu : Fe : Cu to be 24 : 58 : 24. The U.T.S value of the laminated strip is found out to be 273 MPa.

Bibliography

[1] D.R.Lesuer et al. : *Int.Mat.Rev.*, 1996, **41**, (5), 169-195.

[2] D.E.Alman, J.C.Rawers and J.A.Hawk : *Metall.Mater.Trans.A*, 1995, **26A**, 589-599.

[3] V.C.Nardone, J.R.Strife and K.W.Prewo : *Metall.Trans.*, 1991, **22A**, 171-182.

[4] H.S.Ingham,Jr. : *'Composite Engineering Laminates'* (ed. AlbertG.H.Dietz), 1969, Masssachusetts, MIT Press.

[5] V.S. Arunachalam and O.V. Roman : *'Powder metallurgy - Recent advances'*, 1989, India, Oxford & IBH Publishing Co. Pvt. Ltd.

[6] R.K. Dube : *Int. Mater. Rev.*, 1990, **35**, (5), 253.

[7] M.R.Dustoor : *Met. Powder Rep.,* 1982, **37**, 92-93.

[8] D.H.Ro and M.W.Toaz : in *'Progress in Powder Metallurgy'*, vol.38, 311-338, 1982, NJ, Metal Powder Industries Federation. Cited in ref.[6].

[9] O.A.Katrus and G.A.Vinogradov : *Sov.Powder Metall. Met. ceram.*, 1962, **5**, (11), 357-362. Cited in ref.[6].

[10] C.E. Vanburen and H.H. Hirsch : *'Powder Metallurgy'*, (ed. Werner Leszynski), 1961, 403, New York, Interscience Publishers, Inc.

[11] J. Tengzelius and O. Pettersson : *'Powder Metallurgy - An Overview'*, (ed. I.Jenkins and J.V. Wood), 1991, 114, London, The Institute of Metals.

[12] C. Durdaller : *'Source book in Powder Metallurgy'*, (ed. S. Bradbury), 1979, 198, American Society for Metals.

[13] D.G. Hunt and R. Eborall : *Powder Metall.*, 1960, (5), 1.

[14] G.M. Sturgeon et al. : *Int. J. Powder Metall.*, 1968, **11**, 314.

[15] J. Davies, W.M. Gribbon and A.G. Harries : *Powder Metall.*, 1968, **11**, 295.

[16] J.A. Lund : *J. Met.*, 1958, **10**, (11), 731.

[17] C.H. Weaver et al. : *Int. J. Powder Metall.*, 1972, **8**, 3.

[18] M.N. Rahaman : *'Ceramic Processing and Sintering'*, 1995, 735, New York, Marcel Dekker, Inc.

[19] Z.A. Munir : *Bull. Am. Ceram. Soc.*, 1968, **67**, 342.

[20] U. Anselmi-Tamburini and Z.A. Munir : *J. Appl. Phys.*, 1989, **66**, 5039.

[21] K.A. Philpot, Z.A. Munir and J.B. Holt : *J. Mater. Sci.*, 1987, **22**, 159.

[22] D.E. Alman, J.C. Rawers and J.A. Hawk : *Metall.Mater.Trans.A*, 1995, **26A**, (3), 589.

[23] A.J. Bradley and A.H. Jay : *J. Iron and Steel Inst.*, 1932, **125**, 339.

[24] C. Sykes and J. Bamptylde : *J. of Iron and Steel Inst.*, 1934, **130**, 389.

[25] B.H. Rabin and R.N. Wright : *Metall. Trans. A*, 1991, **22A**, 277.

[26] R.J. Lee : *J. Iron and Steel Inst.*, 1960, **194**, 222.

[27] G.H. Fair and J.V. Wood : *Powder Metall.* 1993, **36**, (2), 123.

[28] H. Okamoto and P.A. Beck : *Metall. Trans.*, 1971, **2**, 569.

[29] W. Justusson, V.F. Zackay and E.R. Morgan : *Trans. ASM*, 1957, **49**, 905.

[30] H. Innoune : *MRS Symp. Proc., 'High Temperature Ordered Intermetallic Alloys'*, (ed. C.C. Koch, C.T. Liu and N.S. Stoloff), 1985, 255, Pittsburg, MRS.

[31] C.G. McKamay, J.A. Horton and C.T. Liu : *MRS Symp. Proc., 'High Temperature Ordered Intermetallic Alloys-II'*, (ed. N.S. Stoloff, C.C. Koch, C.T. Liu and O. Izumi), 1987, 321, Pittsburgh, MRS.

[32] Y. Umakoshi, M. Yamaguchi, Y. Namba and K Murakami : *Acta Metall.*, 1981, **15**, 1345.

[33] N.S. Stoloff and R.G. Davies : *Acta Metall.*, 1964, **12**, 473.

[34] S. Hanada, S. Watanabe, T. Sato and D. Izumi : *Scripta Metall.*, 1981, **15**, 1345.

[35] J. Rawers, G. Slavens, D. Gorier, C. Dogan and R. Doah : *Metall. Mater. Trans. A.* 1996, **27A**, 3126.

[36] R.J. Fortnum and D.E. Mikkola : *Mater. Sci. Eng.*, 1987, **91**, 233.

[37] G. Chen, Y. Huang, W. Yang and Z. Sun : *'Processing, Properties and Applications of Iron Aluminides'*, (ed. J.H. Schneibel and M.A. Crimp), 1994, 131, Pennsylvania, TMS.

[38] R.J. Lynch, L.A. Heldt and W.W. Milligan : *Scripta Metall. Mater.*, 1991, **25**, 2147.

[39] R.J. Lynch, K.A. Gee and L.A. Heldt : *Scripta Metall. Mater.*, 1994, **30**, 945.

[40] J.C.M. Li and C.T. Liu : *Scripta Metall. Mater.*, 1995, **33**, 661.

[41] M.G. Mendiratta, H.M. Kim and H.A. Lipsitt : *Metall. Trans. A.*, 1984, **15A**, 395.

[42] I. Baker : *'Processing, Properties and Applications of Iron Aluminides'*, (ed. J.H.Schneibel and M.A. Crimp), 1994, 101, Pennsylvania, TMS.

[43] T. Yamagata and H. Yoshida : *Mater. Sci. Eng.*, 1973, **12**, 95.

[44] I. Baker and D.J. Gaydosh : *MRS Symp. Proc., 'High Temperature Ordered Intermetallic Alloys II'*, (ed. N.S. Stoloff, C.C. Koch, C.T. Liu and O. Izumi), 1987, 81, 315, Pittsburg, MRS.

[45] D.G. Gaydosh, S.L. Draper and M.V. Nathal : *Metall. Trans. A.*, 1989, **20A**, 1701.

[46] V.K. Sikka : *'Processing, Properties and Applications of Iron Aluminides'*, (ed. J.H.Schneibel and M.A. Crimp), 1994, 6, Pennsylvania, TMS.

[47] J.S. Benjamin and T.E. Volin : *Metall. Trans. A*, 1974, **5A**, 1929.

[48] J.C. Rawers and D.E. Alman : *Compos. Sci. Technol.*, 1995, **54**, (4), 379. (*Metals abstracts*)

[49] D.E. Alman : *Proc. Conf., 'Mechanical Properties and Phase Transformations of Multiphase Intermetallic Alloys'*, 1994, 181, Illinois, USA. (Metals Abstracts)

[50] J. Rawers and K. Perry : *J. Mater. Sci.*, 1996, **31**, 3501.

[51] R.K.Dube and P.K.Bagdi : *Met. Trans.*, 1993, **24A**, 1753.

[52] S.Bhargava and R.K.Dube : *Met. Trans.*, 1988, **19A**, 1205.

[53] Robert B.Ross : *'Metallic Materials'*, 1968, 137, Chapman and Hall Ltd., London.